



UNIVERSITAT DE BARCELONA

Final Degree Project **Biomedical Engineering Degree**

**“Scar conducting channel wall thickness
characterization to predict
arrhythmogenicity during ventricular
tachycardia ablation”**

Barcelona, June 2021

Author: Chaimaa Mouhtadi El Kadaoui

Tutor: Paz Garre Anguera de Sojo

I. ACKNOWLEDGMENTS

I would like to express my gratitude to all the Arrythmia's Unit team for offering me the space and the resources needed for this study. Also, for offering me the opportunity to complete this final degree project in an amazing and impressive place. Specially for their kindness and for helping me and supporting me during the development of the whole project. Particularly to my tutor, for her involvement, dedication and enthusiasm to carry out this study. Also, for her time invested in helping me to solve doubts and problems.

In addition, I would also like to thank all my family and friends for giving me the necessary support to perform the project.

II. ABSTRACT

The obtention of cardiac images before the surgery ablation of ventricular tachycardia is widely used to obtain more and better information from the patient than the information obtained during the procedure. This technique is commonly performed using cardiac magnetic resonance since it allows to study and characterise the tissue, which is crucial to detect quantify scarred tissue and the particular region that triggers the tachycardia.

In this project, the arrhythmogenicity of different conducting channels from patients subjected to ventricular tachycardia ablation has been studied along with their wall thickness in order to assess a correlation using late gadolinium enhancement cardiac magnetic resonance imaging. In addition, the correlation between the left ventricle wall thickness of the conducting channels and the outcome of the cardiac catheter ablation performed from the endocardial region of the heart has also been studied. This project emerges from a previous study performed in the Hospital Clínic de Barcelona that characterized several features of the main conducting channel that triggers the ventricular tachycardia.

To perform this study, the images used and the information regarding the arrhythmogenic conducting channel of every patient were obtained from the previous research, using 26 patients for the main objective of this project and using 10 of them for the study of the outcome of the ventricular tachycardia ablation. The study of the wall thickness and the visualization of the conducting channels were performed using *ADAS 3D* software.

Results showed that there was not a significative difference between the wall thickness from arrhythmogenic conducting channels and from the non-arrhythmogenic conducting channels within the patients studied but it is important to highlight that the p-value obtained was too large, which might have been caused by the lack of patients to include to this study. However, an interesting distribution of the arrhythmogenic conducting channel was noticed in the inferior-septum region of the heart, which is interesting to study further in the future using more patients and, hence, more conducting channels to study.

To conclude, it is important to highlight the role of technology and biomedical engineering in this field to achieve better image acquisition to improve therapeutical techniques for the patient and this project has contributed to the awareness and the comprehension of the role of a biomedical engineer in a clinical environment.

KEY WORDS

Left ventricle – Conducting Channels – Arrhythmogenicity – Ablation – Wall thickness – Ventricular tachycardia

III. LIST OF FIGURES

Figure 1: Diagram representing a single circuit of reentry that initiates with unidirectional block [7]	6
Figure 2: Anatomical labyrinth circuit, created by strands of viable myocardium within the scar, with potential for multiple re-entry circuits [7]	6
Figure 3: Activation map with catheter at the site of termination [17]	8
Figure 4: Acquisition strategy for the modified Look-Locker sequence (MOLLI) [64]	12
Figure 5: Representation of the gadolinium molecules distribution on different tissues [58]	13
Figure 6: Representation of the comparison of fibrotic (in red) and normal (in blue) myocardium in LGE-CMR imaging after contrast injection [58]	13
Figure 7: Comparison of arrhythmogenic substrate characterization with the pixel signal intensity map derived from the LGE-CMR (left) and the EAM (right) [58]	14
Figure 8: An example of ischemic cardiomyopathy with apical thrombus in early gadolinium enhancement and LGE images [23]	14
Figure 9: A) Main protocol for LVF and scar quantification B) Incorporation of myocardial stress perfusion to the protocol in A). SAX: short axis; LAX: long axis [27]	15
Figure 10: An example of ischemic cardiomyopathy with apical thrombus adjacent to full-thickness myocardial scar [27]	15
Figure 11: A) Ripple artifacts (red arrow) formed in healthy volunteers with an ICD attached to the left shoulder using old wideband 3D LGE sequence. B) Artifact reduced (green arrow) using the modified 3D LGE sequence in the same volunteers with an ICD attached to them [33]	16
Figure 12: LV segmentation by endocardial and epicardial contours in long-axis and short-axis [34]	17
Figure 13: Myocardial characterization in an ischemic patient. A) Short-axis view of the image, showing in purple the healthy tissue, in green the BZ and in red the scarred tissue. B) 3D reconstruction of the LV using pixel signal intensity information [6]	17
Figure 14: The network architecture. A fully convolutional network (FCN) takes the CMR image as input, learns image features through a series of convolutions, concatenates multi-scale features and finally predicts a pixelwise image segmentation [38]	18
Figure 15: Proposed approach starting with an automatic CNN segmentation of CMR images combined with assessment of segmentation uncertainties. Then, detection of image regions containing segmentation failures using CNN taking CMR images and segmentation uncertainties as input [41]	19
Figure 16: Maximum LVWT by CMR on short axis measured in a patient with hypertrophic cardiomyopathy. In red the endocardial surface is delimited and in green the epicardial surface is delimited [65]	19
Figure 17: The AHA 17-segment model [66]	20
Figure 18: The flowchart consists of motion tracking, spatial normalisation and motion-driven parcellation [43]	20
Figure 19: Transaxial CT image showing the left atrium, right atrium, right ventricle and left ventricle [56]	26
Figure 20: Screen shot of ADAS 3D LV showing a CC in white, scar core volume in red, BZ in orange and healthy tissue in blue in the 10% layer of the LV (the most endocardial layer) and the correspondence between a point in the 3D view and its position in the MRI [58]	28
Figure 21: Example of Segment CMR interface [60]	29
Figure 22: Principal screen of ADAS 3D software [59] Figure 23: Analysis selector [59]	33
Figure 24: First step of CMR LV segmentation, consisting on start generating the model by using four landmarks [59]	34
Figure 25: Screenshot of the second step for segmentation, slice-based adjustment, in ADAS 3D [59] ..	34
Figure 26: Screenshot of the third step for segmentation, model adjustment, in ADAS 3D [59]	35

Figure 27: Representation of the 3D visualization and features in ADAS 3D interface characterising the LV myocardial and showing the healthy tissue (in blue) and the scarred tissue (in red). Screenshot taken by the author of this document	36
Figure 28: Representation of one CC visualization and the AHA segments. Screenshot taken for the author of this document	36
Figure 29: Representation of the LV, CC, AHA segments, core tissue in LV, RV and aorta in ADAS 3D. Screenshot taken by the author of this document	37
Figure 30: Illustration of the LV Wall Thickness representing in blue the thicker areas and in orange the thinner areas. The corresponding AHA segments are also shown by ADAS 3D. Screenshot taken by the author of this document	38
Figure 31: Numeric data representation of the minimum, maximum, mean and standard deviation LV Wall Thickness values of every segment. Screenshot taken by the author of this document	38
Figure 32: Comparison of the wall thickness distribution by type of CC in which 0 represents the non-arrhythmogenic CC and 1 represents the arrhythmogenic CC.....	39
Figure 33: Distribution of the arrhythmogenic and non arrhythmogenic CC in the LV by segments, where 0 represents the non arrhythmogenic CC and 1 represents the arrhythmogenic CC.....	39
Figure 34: Inferoseptal region of the left ventricle containing one CC. Screenshot taken from the author of this document.....	40
Figure 35: Representation of the inferoseptal region of the LV in a 4 heart chambers view [63]	41
Figure 36: GANTT diagram of the project	44

IV. LIST OF TABLES

Table 1: Summary of benefits of CMR guided VT ablation [18]	10
Table 2: Resume of ADAS 3D relevant information [58] [59]	28
Table 3: Resume of Segment CMR relevant information [60]	29
Table 4: Summary of the patients used for this study	32
Table 5: Resume of relevant T-test results	39
Table 6: Project tasks with the corresponding duration	43
Table 7: SWOT analysis.....	45
Table 8: Resume of the total costs of this project.....	46

V. GLOSSARY OF TERMS

VT: Ventricular tachycardia

VF: Ventricular fibrillation

SCD: Sudden cardiac death

CC: Conducting channel

EP: electrophysiological study

CT: Computed tomography

MRI: Magnetic resonance image/imaging

DE-MRI: Delayed enhancement magnetic resonance image

CMR: Cardiac magnetic resonance

LGE-CMR: Late gadolinium enhancement cardiac magnetic resonance

MI: Myocardial infraction

EAM: Electroanatomical map

LV: Left ventricle

RV: Right ventricle

LVWT: Left ventricle wall thickness

BZ: Border zone

ICD: Implantable cardioverter defibrillator

RF: Radiofrequency

bSSFP: Balanced Steady-State Free Precession

GRE: Gradient echo

MRP: Myocardial perfusion reserve

MOLLI: Modified Look-Locker inversion recovery

LVF: Left ventricle function

SAX: Short axis

LAX: Long axis

WB LGE: Wideband late gadolinium enhancement imaging

ROI: Region of interest

FCN: Fully convolutional network

DSC: Dice similarity coefficient

CNN: Convolutional neural network

SVM: Support vector machines
FWHM: Full width at half maximum
STFM: Signal threshold to reference mean
MPI: Maximum pixel intensity
AHA: American Heart Association
ESC: European Society of Cardiology
DOI: Declaration of interest
EHRA: European Heart Rhythm Association
ERTC: EHRA Recognised Training Centers
SCMR: Society of Cardiovascular Magnetic Resonance
LA: Left atrium



VI. TABLE OF CONTENTS

I. ACKNOWLEDGMENTS	I
II. ABSTRACT	II
III. LIST OF FIGURES	III
IV. LIST OF TABLES.....	V
V. GLOSSARY OF TERMS	VI
1. INTRODUCTION.....	1
1.1. Objectives	2
1.2. Methodology	2
1.3. Scope and limitations	3
1.4. Location of the project	4
2. BACKGROUND	5
2.1. State of the art.....	5
2.1.1. Mechanisms	5
2.1.2. Ablation	6
2.1.3. MRI implementation.....	9
2.1.4. Segmentation	16
2.2. State of the situation.....	21
3. MARKET ANALYSIS	22
3.1. VT and CMR research	22
3.2. Segmentation market	23
3.3. CMR market.....	24
3.4. Future perspective of the market	25
4. CONCEPTION ENGINEERING	26
4.1. Study of solutions	26
4.1.1. Type of medical image	26
4.1.2. Segmentation softwares	27
4.1.3. Statistical analysis softwares.....	29
4.2. Proposed solutions	30
5. DETAILED ENGINEERING	32
5.1. Data	32
5.2. Methodology	32
5.3. Results.....	38
5.4. Discussion	40
6. EXECUTION CHRONOGRAM	42



6.1. Definition of tasks and timing	42
6.2. GANTT diagram	43
7. TECHNICAL FEASIBILITY	44
7.1. Strengths.....	44
7.2. Weaknesses	44
7.3. Opportunities	45
7.4. Threats	45
8. ECONOMICAL FEASIBILITY	46
9. NORMATIVE AND LEGAL ASPECTS	47
10. CONCLUSIONS.....	48
11. REFERENCES	49
12. APPENDIX.....	55
12.1. Theoretical concepts	55
12.2. Tables used to compute <i>Figure 33</i>	56

1. INTRODUCTION

Ventricular tachycardia (VT) is a serious heart condition in which the heart rhythm accelerates and does not allow the heart to pump blood properly to the rest of the body. Thus, this condition can produce important effects and symptoms to the patient that can lead to syncope and ventricular fibrillation (VF), which produces eventually sudden cardiac death (SCD).

Its incidence has not been fully estimated but, since VF is responsible for nearly 70% of cases of cardiac arrest [1] for 50% of the cardiac deaths, the impact of VT can be estimated. VT is a highly frequent condition in developed countries, and it is more recurrent in male since ischemic heart disease is more prevalent in this group. Additionally, VT related to ischemic heart disease's incidence increases with age independently from the patient's sex as the prevalence of ischemic heart disease increases [2].

Scar-mediated VT can be treated with substrate-based ablation in order to eradicate the conducting channels (CC) that alter the regular heart stimulation and, thus, the ventricular contraction and the heart rhythm. In order to achieve it, it is important to perform an electrophysiological (EP) study to evaluate the heart's electrical system and locate the focus and the mechanism of the abnormal heart rhythms in order to ablate the main target area that triggers the tachycardia. To study the heart's electrical system, anatomy, tissue and thickness to plan the approach of the procedure, it is important to acquire computational tomography (CT) and magnetic resonance images (MRI). Thus, these images will be processed by imaging softwares that offer tools for detailed fibrosis visualization and 3D reconstruction. This approach is crucial and beneficial in order to obtain information and plan how to perform the procedure and anticipate intraprocedural findings and define strategies, which could improve the duration of a time-consuming procedure.

In the last years, there have been reported important advantages of obtaining pre-procedural images of delayed enhancement MRI (DE-MRI) and incorporating them to mapping systems [3]. It consists of an MRI sequence that acquires the image 10 to 30 minutes after contrast injection. Furthermore, it has been demonstrated that late gadolinium enhancement cardiac magnetic resonance (LGE-CMR) offers high sensitivity and specificity to detect and quantify fibrotic tissue due to myocardial infarction (MI) [4] and it allows the identification of border zones in the ventricular scar tissue, which can be later used to identify CC [5]. Moreover, it has been demonstrated that the ability of detecting fibrosis areas in patients that do not suffer from ischemic heart disease is higher in LGE-CMR obtained before the procedure than in electroanatomical maps (EAM) performed during the procedure [6].

1.1. Objectives

This study is strongly related to a previous research performed by the Arrhythmia's Unit from the Hospital Clínic de Barcelona that is currently in the last phase of its publication, focused on the characterization of an arrhythmogenic CC, which is, among all the CC that a patient suffering from V can present, a single CC that triggers the activation of the general abnormal electricity conduction of the left ventricle (LV) and produces the VT.

Thus, the main objective of this project is to additionally, and following the purpose of the previous research mentioned, assess a correlation between the arrhythmogenicity of a CC and the wall thickness of the areas where the CC is located. Furthermore, succeeding with the study of the left ventricle wall thickness (LVWT), another important objective is to assess a relation between the outcome of the catheter ablation and the LVWT.

An important matter regarding the wall thickness and the outcome of the catheter ablation is the fact that this procedure is performed mainly from inside the ventricular cavity, so it has direct contact with the endocardium of the LV and an objective of this project is to determine if the LVWT of the region where the CC is located influences the ability of the catheter and its range to perform the ablation from the endocardium.

This project also pretends to highlight the importance of the role of the study performed prior to the cardiac ablation, including the image acquisition, its processing, quality and its accuracy in order to provide all the possible anatomical information of the patient's heart and, thus, offer more and better data and information to grant a better interpretation of the patient's actual conditions before the procedure.

1.2. Methodology

This project was performed after a 240 hours internship at the Arrhythmia's Unit at the Hospital Clínic de Barcelona. This internship was very profitable in order to acquire knowledge about ventricular disorders, their treatments, mechanisms and imaging approaches. Furthermore, it was advantageous to become familiar with the study performed before the cardiac ablation, which includes mainly the imaging study of the patient's heart in order to establish a strategy before proceeding with the ablation.

During this internship, 25 cases of patients suffering from VT were studied in order to investigate the mechanism of their tachycardia using a 3D reconstruction software that allowed the visualization of fibrosis areas and CC in the LV. In addition, the distribution of the re-entry mechanism in every CC was studied. Thus, an important basis regarding VT, CC, magnetic resonance image (MRI) segmentation, 3D visualization, interpretation of the left ventricle imaging and its fibrosis was accomplished. For this reason and following the inception of the paper in which this study is based on, the proposal of this project appeared in order to use the knowledge acquired from this internship and continue the paper.

Hence, after this internship and after the conception of the purpose of this project, the next steps were followed:

- First, a bibliographic research was needed in order to get familiarized with VT mechanisms, the LVWT and with the imaging techniques available to visualize the LV, its fibrosis and CC. In addition, *wall thickness study* and *AHA segments* features offered by ADAS 3D software were also studied before starting with the practical stage in order to acquire practice.
- Regarding the practical phase, it was important to make sure that the data of the patients used were the same as the data used for the previous study in order to work with the same CC defined as arrhythmogenic. Then, with the *SPSS Statistical* software, the number of CC, the AHA segments affected by them and the wall thickness of every AHA segment was registered in order to perform the statistical analysis. In addition, the available information about the same patients regarding the number of CC and the AHA segments affected by them that they presented after the ablation procedure was also registered to the data base.
- Finally, a statistical analysis was performed to obtain the results and their pertinent discussion was accomplished. In the detailed engineering section, it was defined the execution and the results of the practical phase. Then, the execution chronogram, the technical and economic viability were presented in this project, as well as the normative aspects and the pertinent the conclusion.

1.3. Scope and limitations

Depending on the complexity of the case and the distribution of the patient's CC, ablation can last typically 4 hours, but it can take longer depending on the type of the arrhythmia or if the heart presents more than one area of abnormal tissue and other complications that may be encountered during the procedure.

For this reason, anatomical and functional image information will be necessary in order to consider their interpretation and to plan a more accurate strategy for the procedure, anticipate complications and reduce the duration of the procedure and thus, since fluoroscopy is used during ablation, the exposure time to X-ray for both patients and professionals would also be reduced. Therefore, it would be advantageous for both patients and hospitals, including personnel and resources, by performing a more efficient procedure. That said, establishing correlations based on information provided by previous image can help to identify in time the interested CC and the target area and thus, prognosticate and anticipate possible complications and suspect the possible outcome.

However, it is important to spotlight that there has been limited papers studying the LVWT over the years and their main purpose was principally to study its influence in hypertrophic cardiomyopathy, but since the last 5 years, its interest has started to grow and more papers are starting to dedicate their study to LVWT relating it to ventricular arrhythmias, myocardial infraction and ventricular function.

In addition, it is important to highlight that since this study represents a final degree project, it presents relevant limitations, most of them concerning time, its scope and conception. In particular, the number of patients to study for the purpose of this project has limited its scope and accomplishment. This limitation affected the two principal objectives and especially the study of the outcome of the catheter ablation and its correlation with the LVWT since only a more limited number of patients presented available image information after the procedure.



Considering these limitations, the scope of this project includes:

- Literature research of the VT mechanism, electrophysiological study, and therapy.
- Study of different techniques involving cardiac magnetic resonance.
- Analysis of different softwares such as *ADAS 3D* and *Segment CMR* to visualize the left ventricle.
- Study of different possibilities to approach the objectives of this project regarding the assessment of local LVWT.
- Research of the LVWT studies and interest in VT ablation.
- Data acquisition of the interested variables from the patients.
- Statistical analysis of the practical part.
- Discussion of the results obtained and the role of the LVWT in VT pathology and ablation.

1.4. Location of the project

The project presented, including image study and data acquisition, has been accomplished in the Cardiology Department at the Hospital Clínic de Barcelona. Particularly, it was performed next to the electrophysiology rooms of the Arrhythmia's Unit, located on the Sixth Floor, pavilion 3 of the Hospital Clínic de Barcelona.

2. BACKGROUND

As beforementioned, VT is a heart disorder in which the heart rhythm is altered due to abnormal electrical signals in the ventricle. Since the heart beats are no longer organized nor synchronized and the heart rhythm increases, the heart is not able to pump enough the blood to the body. This irregular rhythm lasts only a few seconds, it makes the patient feel palpitations, have chest pain, or feel dizzy. However, they can also last much longer and become life-threatening for the patient, resulting in SCD. VT occurs more frequently in the context of healed myocardial infarction and its incidence has declined from 5% to 1% in the last years as a consequence of a greatest control of myocardial infarctions [7]. However, patients that have suffered from a cardiac arrest have an important risk of experiencing recurrent episodes of VT or even VF [8].

Ventricular arrhythmias in the acute phase of ischemia usually degenerate into ventricular fibrillation, that consists of a random cardiac electrical activity that produces multiple waves through the channels. Thus, the heart does not exactly contract effectively, the blood is not pumped to the rest of the body and the patient dies in minutes since VF leads to cardiac arrest. Spontaneous VF is often preceded by VT due to chronic myocardial infarction with ventricular scarring and it occurs because increased oxygen demand during sustained VT can cause degeneration of VT into VF. Besides, acute myocardial ischemia and increased ventricular electrical instability precipitate VF [9].

2.1. State of the art

2.1.1. Mechanisms

VT appears especially after recovery of myocardial infarction since myocardial infarction results in myocardial necrosis in certain regions of the left ventricle, which affects the tissue and its mechanism of contraction of the heart. Thereby, this condition generates a heterogeneity within the ventricle that alters the electrical conductivity of the heart. Thus, it generates scarred tissue, due to the ischemia, and areas that correspond to border zones (BZ) as well, which consist of slow conduction regions that, contrary to the scarred tissue, still present some activity of the electrical conduction. However, this electrical conduction is not appropriate nor coordinated with the rest of the healthy ventricle that presents a proper conduction of the electricity.

The distribution of these border zones is very determinant on the mechanism of the VT. Since they are still able to conduct electricity but, incorrectly, if the BZ is large enough to connect healthy zones, the slow conduction regions that the BZ creates will trigger this incorrect conduction through the rest of the ventricle and, eventually, it will contract more quickly following the nature of the electrical conduction of these BZ. BZ can be located in different areas of the ventricle near or even within the scarred tissue and the slow conduction areas that a BZ configures between healthy areas are called conducting channels. Moreover, a ventricle can present one or several CC, depending on the distribution, heterogeneity, and the size of the scars, BZ and healthy zones.

Thus, VT can be triggered by two types of mechanisms: due to focal activation or due to a re-entry. Focal VT appears mainly due to an abnormal automatism originated in the ischemic border zone in acute ischemia or in cases of healthy heart with monomorphic VT (see 12. Appendix). In this context, the ablation will be performed in this specific area where the focus is localized.

On the other hand, re-entrant VT is the most common sustained arrhythmia, leading to VF [10] in more than 95% of cases [7]. This type of re-entry can be divided into two subclasses: anatomical re-entry and functional re-entry [11].

Functional re-entrant circuit, which is the main type of VT studied for this project, occurs when the conduction of the electric impulse comes across a heterogeneous zone of the ventricle, as mentioned before. In order to initiate re-entrant VT, the impulse needs to arrive to a region of slow conduction in one direction and then, it must be unable to conduct in another region due to the fact that the other areas are blocked conductively. Thus, the impulse will propagate in one direction through the area of slow conduction until it reaches the other side of this region and then it will re-excite the ventricle through the area that was blocked. Finally, this impulse will keep travelling through the ventricle until it finds again the previous entrance of the region of slow conduction to propagate repeatedly the mechanism of this circuit [12] (see *Figure 1*).

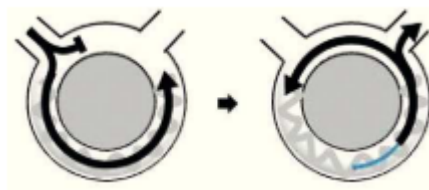


Figure 1: Diagram representing a single circuit of reentry that initiates with unidirectional block [7]

Thus, the main mechanism of scar-related VT consists of a circuit caused by a slow conductive channel of survival myocardial fibers (BZ) characterized by their slow conduction and ability to generate a CC that connects healthy tissue in order to allow the re-entry of the circuit.

Figure 2 represents an example of re-entry circuit created by myocardium within the scar with potential multiple re-entry circuits [13]. Patients that already have structural heart disease tend to have numerous channels [14].



Figure 2: Anatomical labyrinth circuit, created by strands of viable myocardium within the scar, with potential for multiple re-entry circuits [7]

2.1.2. Ablation

Currently, different treatments are available to manage this type of arrhythmia depending on the symptoms, the condition, stability, its mechanism, and other factors regarding the health of the patient and the type of arrhythmia. The treatment can involve pharmacological management, implantable cardioverter-defibrillators (ICD) or ablation, in which this project is focused and interested in.

ICD therapy has been related to mortality reductions of 23 to 55% [7]. Some trials have determined the benefits of using ICD therapies for primary prevention of sudden cardiac death so most patients with scar-related VT use an ICD in order to prevent sudden cardiac death [14].

These types of patients that need ICD therapy present sustained and recurrent VT (see 12. *Appendix*) and catheter ablation is typically performed as an adjunctive therapy [15].

As in pharmacological management, calcium channel blockers and β -blockers (for instance timolol or nadolol) are normally used although they can be associated with side effects and high recurrence rate [12]. However, when they are not effective, other therapies such as ablation are recommended. In order to achieve more effect and reduce the frequency of recurrence of ICD shocks, β -blockers are commonly combined with amiodarone, a III class antiarrhythmic drug that has been associated with adverse effects in 30% of patients, so it can require an alternative therapy as well [15].

Moreover, lidocaine, classified as Ib class, can also be used due to its antiarrhythmic properties and it is useful in VT associated with ischemia or myocardial infarction, but it is less effective in patients with slow and stable VT [14]. Nevertheless, drug therapy has been limited because of adverse effects in long-term therapy [3], as commented, and during the last years there have not appeared important advances in these therapies. Thus, catheter-based ablation has been very recurrent in order to offer new options for this condition.

Catheter ablation is based on delivering radiofrequency energy to the survival myocardial tissue that forms part of the arrhythmogenic focus from the conducting channels. Thus, it generates scars in some specific and previously studied areas of the heart that have been demonstrated to contribute to formatting CC, which are responsible of the malfunctioning of the heart contraction. It is important to consider that, since the main principal of this procedure is to generate fibrosis, after the procedure, the CC target will no longer exist but, since the heterogeneity of the LV will have changed, other regions of slow conduction consisted of BZ that connects healthy tissue can appear and whose significance may have to be assessed.

Radiofrequency catheter ablation has been proven to provide more than 80% of success rate and be very effective [12] and, therefore, it is the most preferred strategy to avoid long-term medical therapy. It is also considered for patients who do not respond well to therapies presented above, do not tolerate drug therapy or are taking incompatible medications [14].

This therapy eliminates VT and it prevents its recurrence. Furthermore, radiofrequency ablation is mostly used along with ICD therapy in case of recurrent VT in order to reduce the amount of ICD therapies needed [16].

As beforementioned, this treatment turns border zones involved in the VT's re-entry to scars so they will not be able to propagate electrical conduction nor be part of a CC. In case of focal VT, since there is a certain area where the automatism and the excitability are altered, the target of the ablation will be this specific area.

However, a re-entry VT can present random areas in the ventricle which contribute to generate these CC that induce the tachycardia. For this reason, the patient's heart and myocardial tissue need to be characterized and analysed with an electrophysiological study in order to plan a personalized procedure for the patient. It is important to induce the arrhythmia with a planned electrical stimulation in order to determine its mechanism and circuit. It is accomplished using activation maps, which allow to identify the earliest zone that triggers the initialisation of the VT and the general circuit of the arrhythmia to identify the regions affected by it. They are useful to describe the myocardial activation and identify critical isthmuses in re-entrant VT. In addition, the

assessment of the arrhythmogenic channel, which corresponds to the main causative channel that induces the arrhythmia, is important in order to identify it and accomplish an accurate guidance and strategy for the ablation of the exact target region. The identification of the arrhythmogenic CC is assessed during the procedure using the information provided by the polygraph and the excitation mechanisms observed during the procedure. *Figure 3* shows an activation map obtained during ventricular tachycardia.

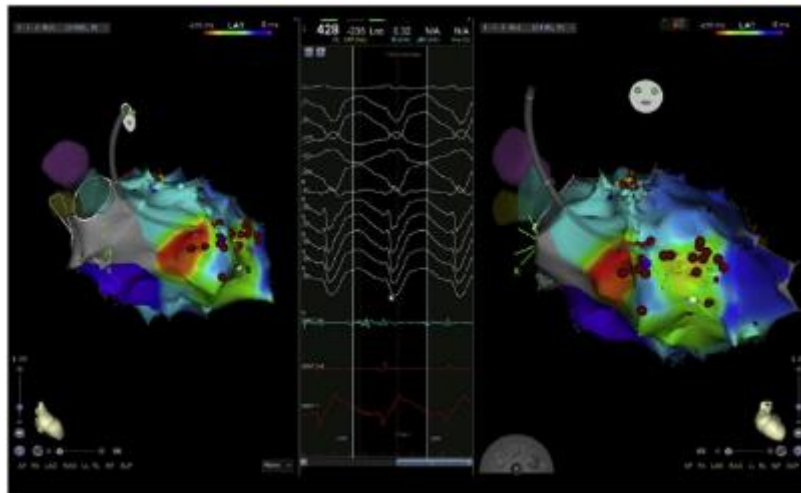


Figure 3: Activation map with catheter at the site of termination [17]

The study before the ablation consists of acquiring MRI images of the patient to obtain detailed information of the heart's anatomy, tissue characterization and thickness and plan which could be the approach during the procedure. It is of main importance since it is necessary to obtain information of the patient before the surgery, which will provide awareness of what type of re-entry will be encountered. In this way, a first idea on how to approach the process is achieved, which is crucial to anticipate intraprocedural findings and define strategies.

Once defined the strategy to follow for the ablation, during the procedure it is necessary to obtain real time image. It is achieved by using fluoroscopy and ECG, which will be used to localize the catheters in the heart by tracking and classifying their signal, and obtaining X-ray image during the procedure (which involves considering security measures). Furthermore, a navigation system is also needed to complement this technique and offer more information by performing an electroanatomical map in 3D. It reconstructs the heart and its cavities in 3D by using electrophysiology catheters. These catheters collect information about the voltage and strength of the bipolar signal of the different areas as they travel through the heart. This signal will present a high or low amplitude depending on the thickness, directionality and electrical activity. Thus, it will be detecting and recording in real time if the tissue where the catheter is located is considered scar, if the value of the voltage obtained in there is lower than 0.5mV, or healthy, if the value obtained is higher than 1.5mV. This tissue characterization technique using voltage information is useful to interpretate if the tissue corresponds to scar because in this case it will present low voltage information since its ability to conduct electricity is almost nil. Additionally, this information will be transformed into a colour code and the system will use it to create the 3D anatomy of the cavity discriminating by colour the core tissue, the healthy tissue and the border zones. It commonly also offers the possibility to mark points of interest in the three-dimensional map, which will be used to plan blocking lines, used as targets for the ablation procedure, to perform during the surgery in order to block the conduction of the CC that cause the arrhythmia.

Finally, after the ablation is performed, a programmed stimulation following a specific protocol is performed to induce VT to evaluate its outcome and assure that the VT/target CC has disappeared.

It is important to highlight that regarding the image obtention during the procedure, this process is time consuming, so it is essential to integrate previous images of the patient obtained by MRI in the navigation system in order to rely on them while real time image information is obtained.

2.1.3. MRI implementation

As mentioned, the most common technique used for diagnostic and management strategy is computed tomography (CT) and cardiac magnetic resonance (CMR) imaging. They provide information about the anatomy and functionality of the heart and determine which patients have risk of inducible VT/VF according to the size of the scar, given by the MRI. Besides, they offer channel identification and characterization. CT uses X-rays to enhance hard tissues and bones whereas MRI allows tissue characterization and anatomical visualization by highlighting soft tissues such like muscle and vessels and it allows to distinguish scarred tissue, measure blood flow and more characteristics that can be obtained from the magnetic relaxation properties. In addition, an MRI study provides information about the tissue's morphology, function, and other type of information to detect thrombus and obstructions, in case of CMR. However, its investigation and application were delayed in comparison with MRI applications in other organs due to the complication that CMR imaging presents regarding the constant movement of the heart, blood and subjacent structures. Different MRI sequences have been implemented and new sequences can be investigated in order to acquire cardiac images the sequence used will depend on the application, therefore, information about the parameters implied in the different sequence pulses that exist is important in order to use accurately this image technique and achieve the maximum possible quality.

The main role of these techniques is to guide catheter ablation of VT as a complement for 3D EAM. Therefore, image techniques that allow myocardial scar characterization before the procedure are helpful to determine the best planning for the ablation and to focus the EAM to actual regions of interest in order to perform an efficient ablation with better outcomes. Hence, since CMR uses powerful magnetic fields and radiofrequency (RF) pulses, it does not use X-rays so it is considered an impressing and promising technique and its implementation should be expanded and upgraded in the future.

Conventional 3D EAMs generated during ablation procedures may present some limitations for heart characterization due to poor catheter contact with the tissue, which may result on false interpretation of low voltage areas corresponding to scar tissue [6]. Moreover, EAM may implicate some other limitations, for instance, limited information on deep tissue or tissue that is located in a poor accessibility area. Additionally, achieving a high precision EAM is time consuming, as mentioned, and it requires experience [6], so a complementary technique that provides similar but more accurate information than EAM is necessary in order to combine previous and real-time information of the patient and perform the procedure in a more accurate way besides offering information prior to the procedure to plan the process, as beforementioned. *Table 1* resumes the benefits of performing VT ablation CMR guided as in ablation applications during the intervention, RF delivery time, inducibility of the arrhythmia right after the ablation to evaluate the outcome and recurrence rate.

Indicator	VT ablation non-CMR guided (105 patients)	VT ablation CMR-guided (54 patients)
RF applications per patient	36 ± 18 applications	28 ± 18 applications
RF delivery time per patient	27 ± 16 minutes	19 ± 12 minutes
Inducibility of VT	51%	32%
Recurrence rate after 20 months	44%	19%

Table 1: Summary of benefits of CMR guided VT ablation [18]

The first cardiac magnetic resonance image was obtained using an intravenous administration of paramagnetic $MnCl_2$ in animals in order to study left anterior descending coronary ligation since it was known that manganese ion was deposit in the myocardium. Since 1970, CMR started to develop, progress, and gain more interest. In 1980, heart imaging progressed significantly by assessing cardiac morphology and characterization with MRI weighted in T1 and T2. Then, with the introduction of the use of contrast agents for this type of imaging a decade later, it started to achieve more value because it presented the possibility to detect myocardial scar [19]. As mentioned earlier, unlike CT, CMR does not present ionization properties and, additionally, its important advances have been developed recently. Moreover, the contrast agents used are generally safe, except in patients with kidney or liver related conditions, so this technique is becoming an interesting and very promising tool that nowadays it continues to evolve technically and it will sure keep developing in the future in order to improve it and offer more advantageous features. At the present, magnetic field strength for cardiovascular imaging has increased and most MRI systems in clinical use are between 1.5T but mostly 3T, which offers better spatial resolution for better detection of BZ [20].

Thus, it is evident that CMR presents several advantages against other cardiac imaging techniques. This modality is used principally in investigations regarding ischaemic heart diseases because it has become a precise anatomical delineator of cardiac structures, an important tool to characterize myocardial tissue and it can be performed in main hospitals. It also offers other interesting features such as accurate measurements of ventricular volumes and myocardial mass [6]. An important quality that CMR presents is that it can be used for different purposes and approaches regarding the cardiovascular system due to its compatibility to be performed with different pulse sequences developed to assess different cardiac features. Some of them are presented below:

- **Cine imaging:**

Cine CMR consists of acquiring the same slice position repeatedly in an area of interest at different phases of the cardiac cycle in order to capture motion [21]. It is mainly used to assess LV and right ventricle (RV) functionality and fibrosis. This technique offers high tissue contrast and it is the gold standard of quantification and accurate imaging modality to assess ventricular volumes and function [22], as well as LV mass. Cine imaging is also used to determine wall thickness and contractility. In addition, it enables inspection of cardiac structure and wall motion and reproductivity.

Thereby, this technique provides information about parameters that establishes the basis of clinical decisions and treatment guidance [23].

For this technique, balanced Steady-State Free Precession (bSSFP) sequence is used because of its exceptional contrast between myocardium and blood pool, which consists on the ventricle cavity, in this case, that it is filled with blood so it does not include myocardium and it is used as a reference for contrast. However, in case an artifact is present, gradient echo cine (GRE) imaging is preferred [24], which allows fast cine acquisition with high resolution and it generates bright-blood images.

- **Black or dark blood sequence imaging:**

This technique uses double inversion recovery preparation pulses to suppress the blood signal and highlight and delineate the vascular and myocardial structures with the blood darkened.

It is used to detect vascular and myocardial abnormalities such as congenital anomalies, myocarditis and cardiovascular tumours [25]. In addition, it allows blood flow quantitation and tissue characterization by highlighting signals from areas of low flow and representing with low signal regions with intramyocardial haemorrhage [24]. Furthermore, it is considered the best modality to assess pericardial thickening [26].

Since T1 and T2 black-blood sequences require long acquisition times, which implies slow blood flow artefacts and inadequate blood signal suppression, this method has been replaced by GRE and bSSFP sequences [23].

- **Stress (and rest) perfusion CMR or First-pass contrast-enhanced**

This imaging technique is useful to assess the microcirculation of the myocardium. Using a T1-weighted GRE sequence in order to implement dynamic imaging after an injection of gadolinium as a contrast agent, dynamic images are acquired. When gadolinium circulates in the myocardium, the T1 time is reduced, and the myocardium is enhanced depending on the concentration of gadolinium. This technique is performed under rest and under stress state, which is induced pharmacologically by injecting a vasodilator that increases perfusion such as adenosine. Dobutamine can also be used as an alternative to adenosine to assess myocardial ischemia by detecting stress-induced wall motion abnormalities and, besides, it is considered to be a better method to perform this technique. However, it involves more risks than using adenosine, for instance hypotension and ventricular arrhythmias. In order to determine whether myocardium is considered normal or ischemic, a ratio of perfusion at stress state and rest state is defined. If the value of this ratio, which is called myocardial perfusion reserve (MRP), is higher than 2, it is considered normal myocardium and if the value is lower than 1.5, it is considered ischemic [25]. This technique has been confirmed to be a validated method to verify myocardial ischemia.

To perform this technique, stress perfusion must be performed before rest perfusion because gadolinium accumulates in regions of scar, which impedes the measure of hypoperfusion.. [27].

Frist-pass perfusion imaging allows the detection of tumour vascularity and it has been shown to offer accurate diagnostic of coronary artery disease [25]. This technique can be combined with other techniques used for different purposes in order to determine the presence of inducible ischemia.

Nevertheless, the most common CMR techniques for scar imaging are late gadolinium enhancement CMR (LGE-CMR) and T1 mapping.

T1 mapping is a technique that represents a two-dimensional slice image (see *Figure 4*) where each pixel displays the T1 relaxation time, which is specific on the type of the tissue. T1 map can differentiate acute from chronic myocardial infarction due to its sensibility to detect the edemas resulting from acute injury since they contain water. Furthermore, it can determine the area of myocardial ischemia and, moreover, the area corresponding to the tissue at risk of irreversible damage after reperfusion interventions [28]. Therefore, it is used for myocardial tissue characterization. T1 reflects changes in extracellular and intracellular compartments and, in addition to water, it is also affected by collagen, lipid, proteins and iron content.

T1 mapping can assess the degree of myocardial fibrosis invisible to LGE-CMR. Different acquisition methods based on bSSFP sequences can be used but the modified Look-Locker inversion recovery (MOLLI) is commonly used to quantify T1 of the myocardium. This technique can be performed using a contrast agent such as gadolinium. An increased myocardial T1 time before contrast administration has been described in myocarditis and hypertrophic cardiomyopathy among other pathologies. On the contrary, regarding iron concentration, it will show a decreased pre-contrast myocardial T1 time [25].

Even though post-contrast myocardial T1 time may be affected by different factors, some studies propose to measure the change in T1 time in pre and post-contrast injection in order to measure the extracellular volume fraction, which some studies relate its increased values to diastolic dysfunction and diffuse myocardial fibrosis [25]. An important weakness of this technique is its sensitivity to heart rate and image noise [29].

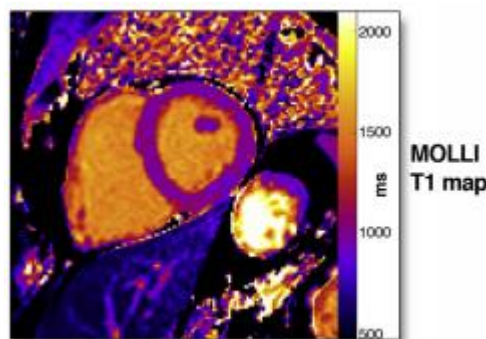


Figure 4: Acquisition strategy for the modified Look-Locker sequence (MOLLI) [64]

LGE-CMR is based on the use of gadolinium as a contrast agent in order to highlight areas of fibrosis. This contrast agent is injected 10-30 minutes before the acquisition. It is used for cardiac tissue characterization due to gadolinium's property regarding to its interaction with the tissue, specifically the time in which gadolinium remains in the tissue. In healthy myocardium, it remains in the tissue for a few minutes while in scarred tissue the speed at which the gadolinium leaves the tissue is much slower, so it is retained there for a longer time. It is performed using a T1-weighted rapid GRE sequence combined with an inversion recovery pre-pulse [25].

In *Figure 5* it can be seen that these gadolinium molecules can accumulate in extracellular spaces and, hence, in case of scarred tissue and since it presents larger extracellular space due to the abnormality of the tissue, the concentration of molecules there will leave at a slow rate. On the contrary, in case of healthy and normal myocardium, where the accessible extracellular space is more limited, the molecules can barely enter the myocardial cells and they will disappear faster and easily. Thus, the contrast in signal shows a difference between fibrotic tissue and normal myocardium, representing scarred tissue in white and normal tissue in black (see *Figure 6*).

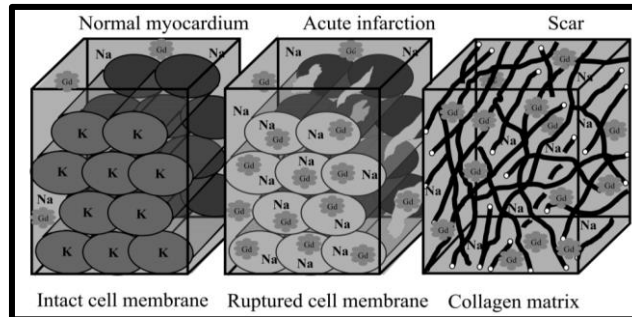


Figure 5: Representation of the gadolinium molecules distribution on different tissues [58]

Thus, gadolinium shortens the T1 time in tissues where it is accumulated, which will provide a high-intensity signal on T1-weighted imaging [30]. *Figure 6* describes the effect of contrast injection on the concentration curves of the gadolinium after a delayed enhancement. It can be noticed that after a certain time the fibrotic myocardium in this type of MRI is highlighted in white while normal tissue is showed in black (see *Figure 6*). Therefore, selecting the correct time to acquire the images is essential to highlight the fibrotic areas in order to differentiate them from the normal tissue. On the contrary, the images obtained will not show appropriately the fibrosis quantification and they will have to be interpreted differently.

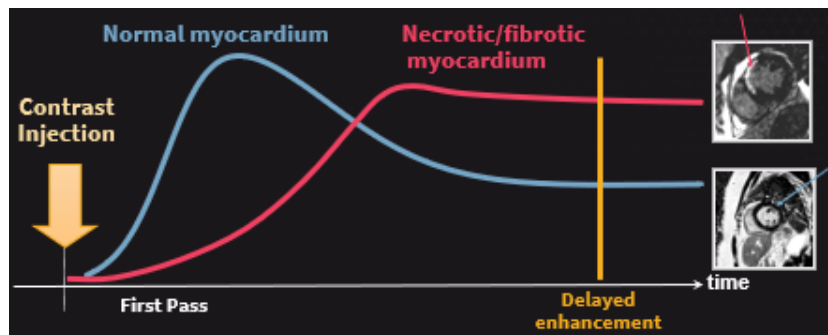


Figure 6: Representation of the comparison of fibrotic (in red) and normal (in blue) myocardium in LGE-CMR imaging after contrast injection [58]

As mentioned, the main role of pre-procedural imaging such as LGE-CMR is to aid VT catheter ablation. Therefore, an accurate image registration for CMR images in navigation systems is required. Almost all the navigation systems offer an automated registration algorithm in order to reduce the distance from an image imported to the EAM (see *Figure 7*) [6]. Thus, it is important to find an appropriate correlation between the bipolar signal amplitude values and the LGR-CMR relation used to discriminate whether a region corresponds to scarred tissue, BZ or healthy tissue, which will also depend on the contrast administration and acquisition time since it can change the outcome if the acquisition of LGE-CMR images is performed earlier, on time or tardy. For instance, Caixal G. et al [31] demonstrated that LGE-CMR intensity correlates to bipolar

voltage and to conduction velocity as well, in a research studying the accuracy of left atrial fibrosis detection with CMR.

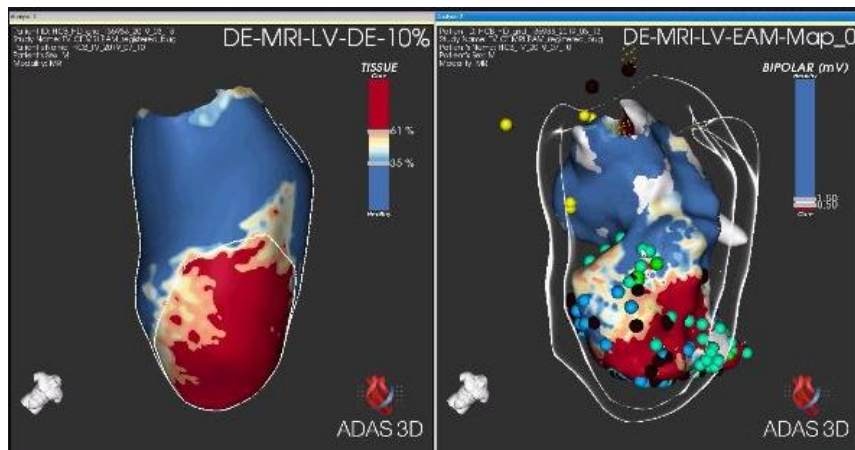


Figure 7: Comparison of arrhythmogenic substrate characterization with the pixel signal intensity map derived from the LGE-CMR (left) and the EAM (right) [58]

Therefore, its performance will rely on operators to assure a correct concentration of gadolinium to inject and a correct inversion time in order to suppress the signal from the normal myocardium, which may be necessary to adjust several times during acquisition of LGE-MRI. Nowadays, a sequence named phase-sensitive inversion recovery (PSIR) has been developed to solve this problem [25].

Figure 8 represents an exemplification of two extreme cases of time acquisition, which represent two methods of image acquisition that provide two different images that require different interpretation.

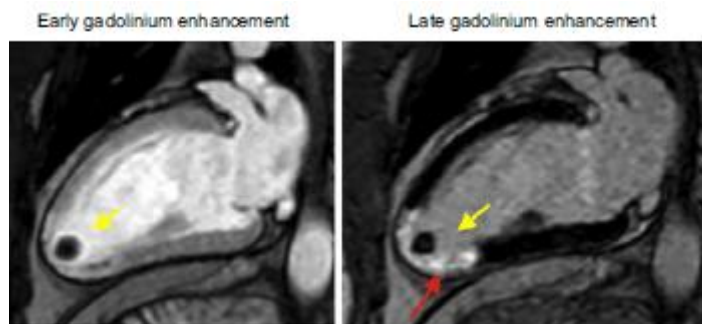


Figure 8: An example of ischemic cardiomyopathy with apical thrombus in early gadolinium enhancement and LGE images [23]

Figure 9 shows two basic CMR protocols followed in clinical routines. The first one involves the use of cine imaging and LGE to assess LV function (LVF) and fibrosis. The second one also includes myocardial stress perfusion in cases in which myocardial ischemia is suggested or when it is needed for guidance to coronary intervention.

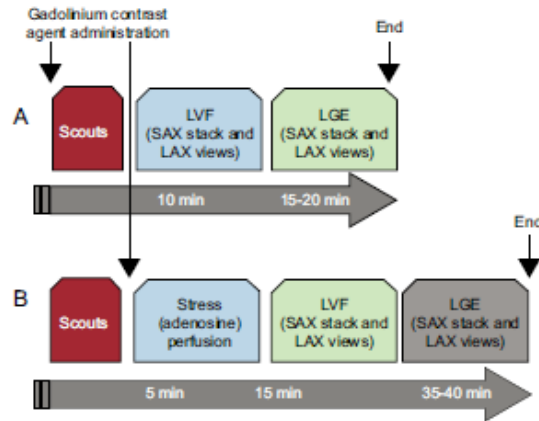


Figure 9: A) Main protocol for LVF and scar quantification B) Incorporation of myocardial stress perfusion to the protocol in A).
 SAX: short axis; LAX: long axis [27]

Figure 10 represents the evolution of cine, stress perfusion and LGE images along a short axis slice.

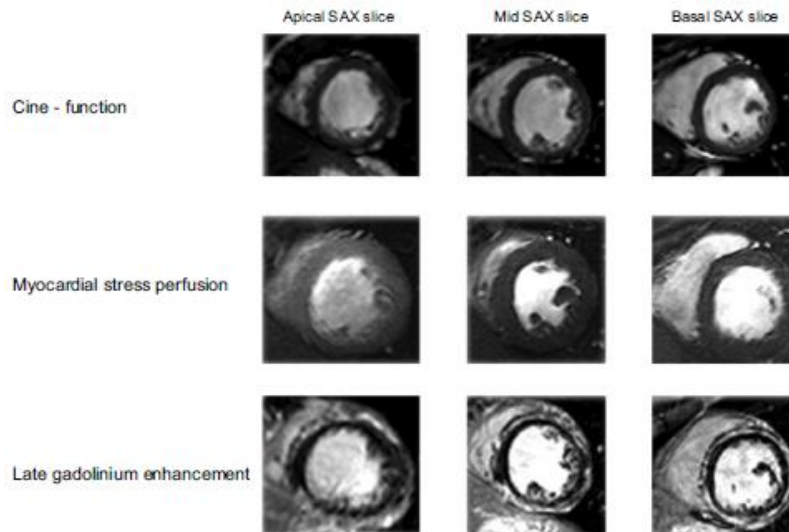


Figure 10: An example of ischemic cardiomyopathy with apical thrombus adjacent to full-thickness myocardial scar [27]

The combination of these techniques explained above (cine imaging, stress and rest perfusion and LGE-CMR) allows the quantification of ischemic tissue and it also allows to define the myocardial delimitation of scar to assess myocardial viability [26].

Furthermore, LGE-CMR combined with stress-induced contractility reserve has been shown to be useful in order to determine hibernating myocardium [25]. In addition, CMR T1 mapping and LGE-CMR combined have shown to offer complete assessment of myocardial scar [30]. For this reason, LGE-CMR has become an outstanding imaging tool in the last years to overcome some of the EAM limitations and to use it as a technique to guide VT catheter ablation as well.

Nevertheless, although the use of MRI is a crucial technique to diagnose and treat VT, an important percentage of patients use implantable devices, such as ICD, which are incompatible with 3T LGE-CMR since it can induce device failure, lead failure and other adverse interactions

[29]. Therefore, it has been studied and implemented **wideband late gadolinium enhancement (WB LGE) imaging**, which uses wide band pulse sequence compatible with ICD [24].

In addition, Roca-Luque I. et al [32] demonstrated that the use of WB LGE cardiac magnetic resonance sequence is suitable for the assessment of myocardial scarring in patients with non-MRI compatible ICD at 1.5T, allowing adequate VT substrate characterization to guide VT ablation with similar accuracy than conventional (3T) LGE-CMR in patients without ICD.

However, this technique used for patients using non-MRI compatible ICD at 1.5T can produce the appearance of image artefacts that can mask scar tissue, which affects the corresponding accurate interpretation, diagnosis, and treatment. To reduce or eliminate device-related image artifact, Rashid S. et al have developed a modified 3D wideband LGE sequence that offers similar image quality compared to conventional 3D LGE-CMR [33].

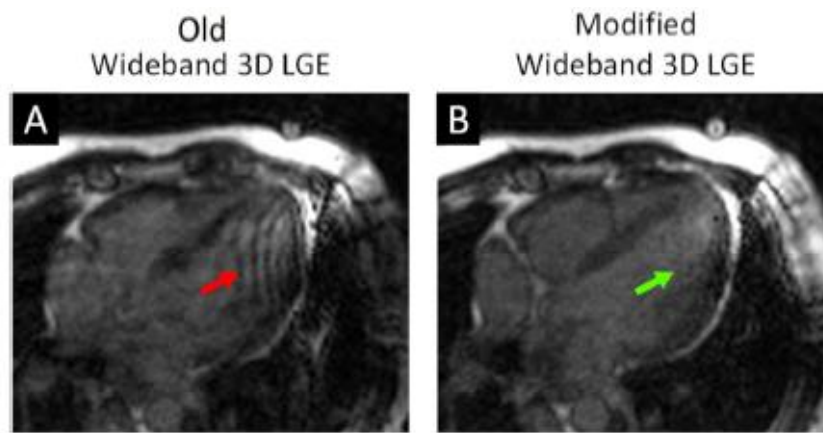


Figure 11: A) Ripple artifacts (red arrow) formed in healthy volunteers with an ICD attached to the left shoulder using old wideband 3D LGE sequence. B) Artifact reduced (green arrow) using the modified 3D LGE sequence in the same volunteers with an ICD attached to them [33]

However, most of the clinical scanners are usually 3T scanners [20] so, efforts to extend this technique to 3T scanners may be important to consider. It is also important since 3T MRI enables higher spatial resolution than 1.5T for better myocardial characterization and detection of CC [20]. In addition, as new MRI-compatible ICD are developed in the market, Ranjan, R. et al [20] demonstrated the feasibility of WB LGE-CMR for imaging ventricular scar without image artefacts induced by these MRI-compatible ICD in 3T. In this study, the effects of these artefacts, such as image distortion and spatial shifts, were minimized by using ultra short echo-time pulse sequences but to confirm these findings, a more exhaustive research would be needed.

2.1.4. Segmentation

2D LGE-CMR has been defined as a reference standard for myocardial scar identification but, 3D LGE-CMR is a recent technique that allows accurate spatial quantification, higher signal intensity and contrast for myocardial fibrosis. It also provides thinner slices compared to 2D imaging, allowing more flexible post-processing and more accurate cardiac features measurements [33].

Image segmentation consists in partitioning a digital image into segments in order to extract a region of interest (ROI) to simplify the representation and visualization of anatomical structures, to delineate pathological regions and to use it for surgical planning and image-guided interventions.

It can be performed through a manual, semiautomatic or automatic process that divides an image into different regions such as organs, tumours or tissue based on specific characteristics. In this project, segmentation refers to detecting the LV contour by defining structures such as the endocardium and epicardium contours and to characterise the myocardial tissue. *Figure 12* represents LV 3D reconstruction based on the definition of endocardial and epicardial contours in LAX and SAX.

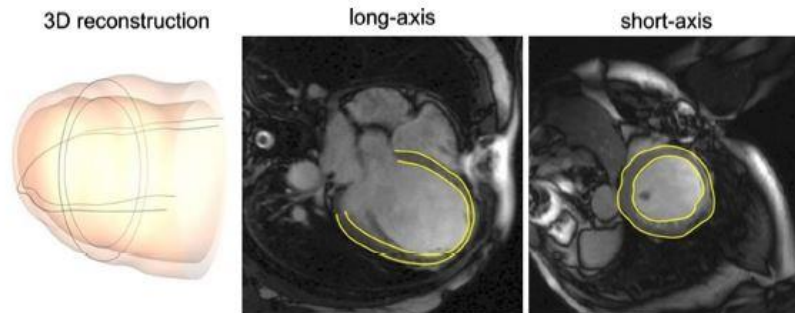


Figure 12: LV segmentation by endocardial and epicardial contours in long-axis and short-axis [34]

To extract the ROI, clustering procedures can be applied. Moreover, intensity or other type of information from the images can be used to apply pixel intensity-threshold-based methods or energy minimization-based methods to segmentate myocardial fibrosis from LGE-CMR images.

Two common cardiac infarct segmentation techniques prior to deep learning-based methods are based on a fixed-model approach, which are **full width at half maximum (FWHM)** and **signal threshold to reference mean (STRM)**. FWHM method consists in using the maximum pixel intensity value in the myocardial boundary as a reference and considering as scar any intensity value that represents the half of the maximum intensity value.

Using the maximum signal intensity (MPI) of the myocardial fibrosis region, which is a modified FWHM method, the threshold used conventionally is to consider BZ from 40 to 60% of MPI, healthy tissue below 40% of MPI and fibrotic tissue above 60% of MPI [5].

In STRM, the intensities are thresholded to a fixed intensity value of standard deviations plus two, three, four, five or six standard deviation (STRM2, STRM3, STRM4, STRM5 and STRM6, respectively) [35] from the mean intensity value of the blood pool [36]. *Figure 13* represents an example of segmentation and it shows endocardial and epicardial contouring in the LGE-CMR image and the corresponding myocardial tissue characterization in a particular slice.

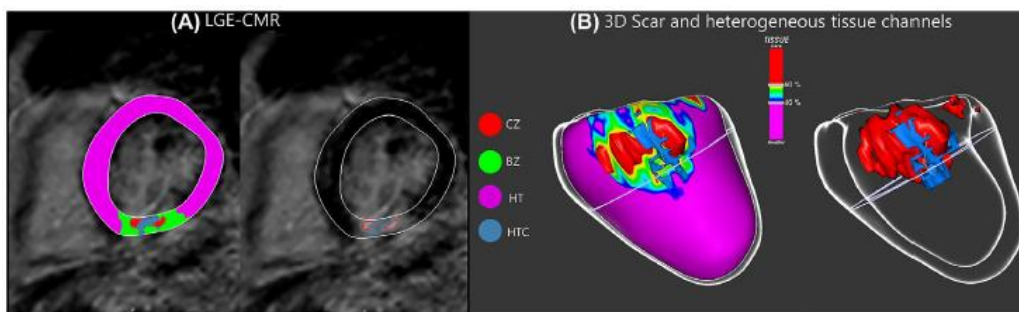


Figure 13: Myocardial characterization in an ischemic patient. A) Short-axis view of the image, showing in purple the healthy tissue, in green the BZ and in red the scarred tissue. B) 3D reconstruction of the LV using pixel signal intensity information [6]

However, segmentation of scar tissue in LGE-CMR can be challenging due to contrast and patient variation, motion blurring, thin wall, etc. For this reason, the interpretation of the quantification of scar can change and affect the appropriate scar threshold and generate variabilities. These methods require a fixed intensity threshold that involves a region-growing process in which seed points have to be defined manually within infarcted regions so that they can be segmented with region-growing. In addition, these methods use simple features such as intensity information, as mentioned, or energy information as well, for instance. They are usually semi-automatic, so they require some manual segmentation of the myocardium in order to define initially contours and structures of the ventricle and the rest of the process is usually automatic.

For this reason, if this process is performed manually or semi-automatically, it may be time consuming, and it is affected by observer variability, so an automated technique may be preferred. Consequently, during the last years an interest for the automatization of this process has grown specially with the progress and the impact of artificial intelligence and particularly deep learning for clinical purposes. Here are exposed two automated LGE-CMR image segmentation techniques based on deep learning:

- Fully convolutional network (FCN):** it consists of a neural network that learns image features and predicts the label class for each pixel by applying different convolutional filters onto an input image [37]. It is used for automated pixelwise image segmentation. This technique provides an accurate segmentation for healthy adult CMR images, but it shows lower performance on patients that suffer from congenital heart diseases [38]. According to Bai et al [37], this method works precisely on a subset of pathological cases and their study demonstrated smaller computer-human difference than human-human difference using a data set of 4.874 subjects. Moreover, Moccia et al [39] obtained a dice similarity coefficient (DSC) of 54% for their FCN strategy for scar segmentation on LGE-CMR images.

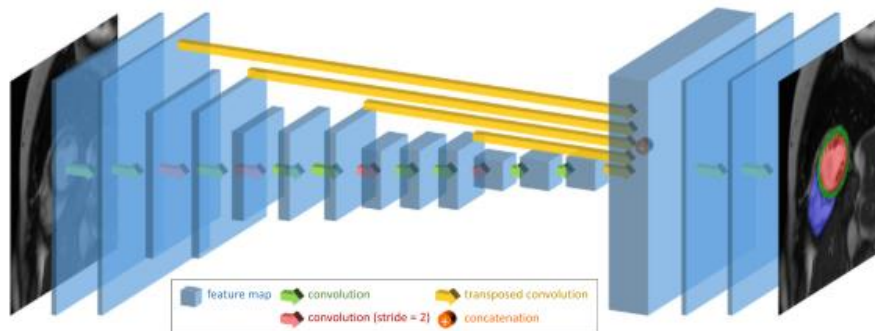


Figure 14: The network architecture. A fully convolutional network (FCN) takes the CMR image as input, learns image features through a series of convolutions, concatenates multi-scale features and finally predicts a pixelwise image segmentation [38]

- Convolutional neural network (CNN):** majority of deep learning-based algorithm use CNN to segment myocardial infraction in LGE-CMR images [35]. It is based on using multiple layers to solve complex data with large feature sizes [37]. Zabihollahy F. et al [40] demonstrated the feasibility of fully automated quantification of LV scarred tissue from 3D LGE-CMR images from 34 patients with ischemic cardiomyopathy with high accuracy and a DSC of 93.6% from pre-segmented LV. In addition, a study performed by Sander J. et al [41] showed that combining automatic segmentation and manual correction of segmentation errors results in higher segmentation performance. *Figure 15* represents the proposed approach.

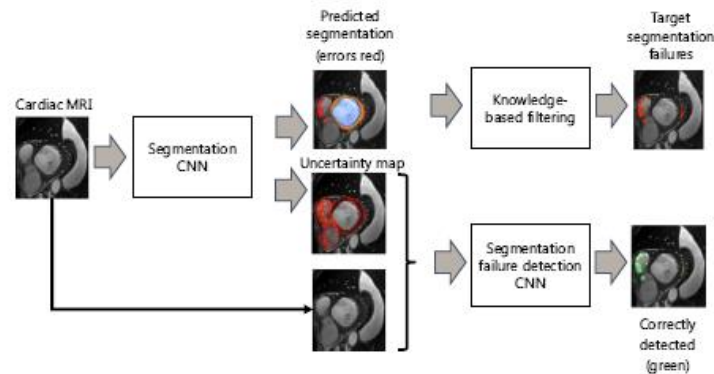


Figure 15: Proposed approach starting with an automatic CNN segmentation of CMR images combined with assessment of segmentation uncertainties. Then, detection of image regions containing segmentation failures using CNN taking CMR images and segmentation uncertainties as input [41]

Regarding the left ventricle wall thickness values, they can be obtained once a good representation of LV epicardial and endocardial borders are achieved since wall thickness is derived from CMR acquisitions, but visual assessment of LV epicardial and endocardial borders implies observer-variability, which involves disadvantages on its analysis.

For this reason, different groups have proposed techniques in order to obtain 3D wall thickness quantification basing on 3D images. Considering the definition of thickness as the distance that separates the epicardial and the endocardial surfaces, this distance can be defined as the minimum distance between surfaces (as seen in *Figure 16*) or as the perpendicular projection between both surfaces, which may not be accurate in case both surfaces are not perfectly perpendicular.

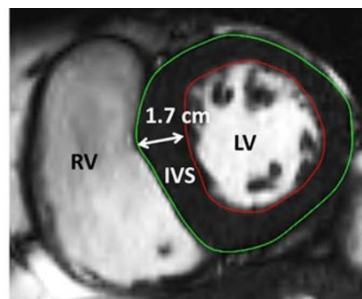


Figure 16: Maximum LVWT by CMR on short axis measured in a patient with hypertrophic cardiomyopathy. In red the endocardial surface is delimited and in green the epicardial surface is delimited [65]

For wall thickness measure, it is assumed that the shape of the myocardium is a circle, so it uses a radial method to calculate the distance between epicardium and endocardium to assess the thickness.

Regarding local assessment of LVWT values, standard 17-segment model defined by the American Heart Association (AHA) is conventionally used. It consists of dividing the LV in 17 segments using criteria based on anatomical structures, which defines 6 basal segments, 6 mid segments, 4 apical segments and 1 apex segment, which, depending on the anatomy, some patients do not present this segment following the AHA segments model.

Figure 17 represents the standardized myocardial segmentation (AHA).

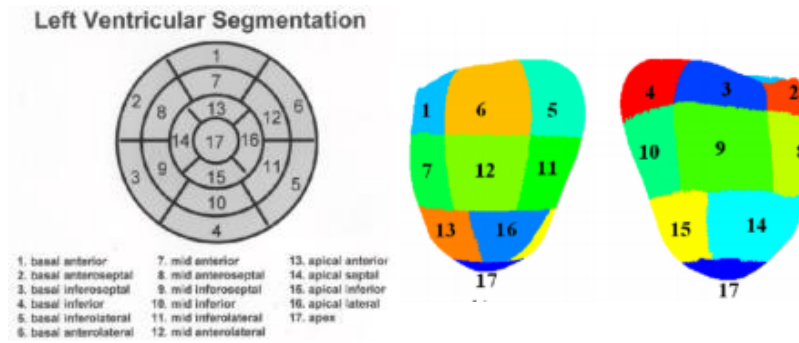


Figure 17: The AHA 17-segment model [66]

However, other models to define LV segments have been studied and proposed using other type of criteria such as the fact that both shape and motion may result changed after myocardial infraction [42]. For instance, a recent research performed by Bai et al. has studied segmentation by cardiac motion since there may exist regions with similar and distinctive motion information. This study has demonstrated that dividing the LV into segments by similar motion behaviour has good reproducibility and can be used to reduce data dimensionality and be applied to cardiac motion analysis [43]. Figure 18 represents the flowchart for the execution of this type of LV model.

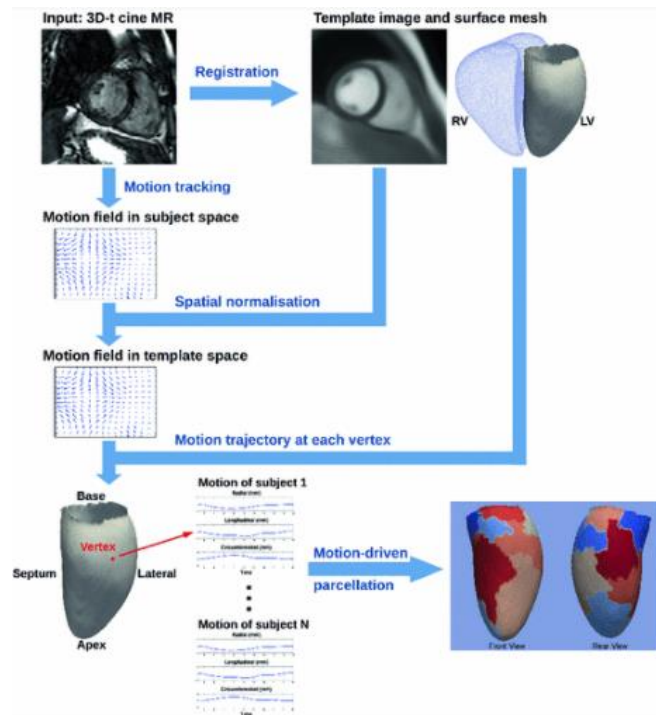


Figure 18: The flowchart consists of motion tracking, spatial normalisation and motion-driven parcellation [43]

2.2. State of the situation

The research carried out by researchers from Arrhythmia's Unit in Hospital Clínic de Barcelona achieved to characterize the arrhythmogenic CC in VT. This research first assessed the arrhythmogenic CC in a series of patients during the electrophysiological study. The patients chosen for the paper were patients in which the process was performed using catheters that offer more points density for mapping, which allowed to obtain more information for the mapping and more facility to perform the procedure. Then, a correlation with the arrhythmogenicity and the length, mass, width, and protectiveness of the arrhythmogenic CC defined was established.

Thus, this project pretends to extend the reach of this recent paper, which, as beforementioned, has not been published yet but its publication is currently in process, by studying the correlation of the LVWT and the arrhythmogenicity of a CC by using the same patients' images and information used on the previous paper. In addition, another purpose for this project is to study the relation between the LVWT of the CC and the outcome of the ablation since most of the procedures only perform the ablation from the endocardial part of the LV.

3. MARKET ANALYSIS

3.1. VT and CMR research

Ventricular tachycardias have been reported since the beginning of the XX century, when, for the first time, an arrhythmia was demonstrated to have its origin in the ventricle, shown by the electrocardiographic description in England and The Netherlands. Ventricular fibrillation was previously recognized as a common terminal condition in dying patients but later, different studies suggested that VT eventually may induce VF. For this reason, an interest for the study of VT started to increase in order to establish its correct diagnosis and study treatments for this condition. Thus, pharmacological, surgical and cardioversion techniques started to develop in order to treat this condition [44].

Regarding current research on this condition, there are different teams and leading research groups and institutions dedicated to arrhythmias and electrophysiology in different countries such as Spain, USA, Singapore, UK, Germany and The Netherlands. For instance, the University of Chicago Medicine's Ventricular Tachycardia Program has been recognized as one of only a few hospitals in the United States that offers the three conventional and commercially available mapping systems technologies used in the United States, and it is specialized in maximizing innovation and advancing VT research by maintaining a data base of outcomes information for ablation procedures. In addition, they are nationally ranked for their specialized epicardial techniques performed during standard endocardial procedure [45].

Penn Cardiac Electrophysiology, from the school of medicine of the University of Pennsylvania, is recognized as a leading centre for research, clinical innovation, and treatment of patients with ventricular arrhythmias. The Penn Ventricular Tachycardia Centre was established in their faculty in 2018 and it focuses on growing global educational efforts related to VT ablation and treatment. In addition, with the collaboration of the Mt. Sinai School of Medicine, it hosts the annual International VT Symposium, considered as a leading VT conference [46].

Regarding organizations and scientific divulgators, the American Heart Association (AHA) is considered as the maximum scientific reference in cardiology in the United States and it defines directrices for medical advances in cardiology internationally. It was founded in 1924 with the purpose of spreading scientific research related with heart diseases. Then, it started to grow, and it started to lead meetings oriented to the cardiovascular health community. Consequently, the association won its first research grant, that helped it to fund more studies, including nine studies that led to the Nobel Prize. AHA has taken part in many important studies over the years, for instance, the first pacemaker implanted and the first successful artificial heart valve replacement. They are also known for publishing guidelines on cardiovascular diseases preventions and standards in basic life support and advanced cardiac life support [47]

The European Society of Cardiology (ESC) is another association that improves the implementation of standards of diagnosis and treatment of cardiovascular diseases. It is a volunteer-led medical society that operates a Declaration of Interest (DOI), improves scientific understanding of the heart, and leads heart congresses.

The European Heart Rhythm Association (EHRA) is an association of the ESC and the European Cardiac Rhythm Management that has more than 3,500 members, including arrhythmologists, electrophysiologists and nurses, that provides education, quality recognition, training and certification to physicians. It also initiates or takes part of research and studies in arrhythmias and publicises scientific information. Its quality seal, named EHRA Recognised Training Centers (ERTC), verifies and highlights efficiency, the use of advanced and uniform teaching techniques, it increases notoriety and attracts fellows and practitioners. In addition, this seal verifies the uniformity of educational tools and standardised practical teaching and it is directed to EP labs and centres [48].

Recently, there has been an important interest in evolving in imaging myocardial fibrosis with CMR, which has improved due to a lot of advances in the last years. CMR has gained an important role in cardiology due to its capacity to offer a deep and exact evaluation of the cardiac function and structure. Currently, two CMR acquisition protocols have been designed and they can be performed in most clinical departments in 20 or 45 minutes. Hence, CMR, over other non-invasive imaging techniques, offers comprehensive, relevant and precise information used to assess accurate diagnosis and prognosis.

Society of Cardiovascular Magnetic Resonance (SCMR) is the principal international organization committed to the development of CMR via research, quality control and training. Their membership includes cardiologists and engineers around the world. This society includes professionals involved with CMR sequence development, preprocedural planning, image acquisition and image interpretation [49].

Its scope has expanded and nowadays the use of 3D CMR can show exactly where the heart is not pumping correctly or help to explain the focus of a heart problem, for instance. In addition, it offers information that allows to decide proper medication or to recommend another medical test. In addition, it allows virtual heart biopsy, visualization and measurement of the blood flow inside the heart muscle, and measurements of tissue properties that are related to diseases [50].

3.2. Segmentation market

As commented earlier, cardiac imaging segmentation consists of delineating the heart chamber contours, particularly the LV, in this context. LV segmentation is a crucial step in order to work with image information and, therefore, an accurate LV contouring is necessary in order to obtain appropriate information as in shape and size. [51].

In general, LV segmentation techniques can be classified in manual, semi-automatic and automatic. Manually segmentation is time-consuming, and it is subjected to inter and intra observer variabilities. Therefore, nowadays, several commercial segmentation softwares offer semi-automatic or even automatic algorithms approaches. Semi-automatic segmentation softwares require limited user interactions to establish particular landmarks or other requirements in order to guide the segmentation process. However, fully automated cardiac segmentation methods, for instance, are not accurate enough, basing on DSC [52].

Circle Cardiovascular Imaging Inc. is leading the emerging market of cardiovascular imaging and ablation planning with over a decade of experience. It develops a cardiovascular post-processing software that allows visualization and analysis of CMR and CT images. It offers cvi42, a leading cardiovascular imaging software for cardiac MR, cardiac CT and cardiac interventional planning

application that can be used in different fields such as heart function assessment, flow quantification, tissue and perfusion characterization, anatomy visualization and it also offers tools for angiography. It provides tools to accurately quantify and diagnose cardiovascular diseases and to improve surgical outcomes. It uses machine learning to offer improved imaging features and precision. In 2019, Circle Cardiovascular Imaging and Galgo Medical SL, a company that developed an imaging post-processing software for electrophysiologists focused on the identification of arrhythmia substrate and the planning of ablation procedures using MRI and CT images, announced that they would start distributing, commercialising, and developing ADAS 3D software together. Since then, cvi42 integrates ADAS 3D Medical to enable pre-procedural planning by quantifying LV and left atria fibrosis and LVWT and displaying the surrounding anatomical structures. Thus, the intention of Circle Cardiovascular Imaging is to make the ADAS 3D software more widely available for electrophysiologists [53].

ADAS 3D is a semi-automatic segmentation and post-processing software for pre-intervention use for LGE-CMR and CT images that detects automatically scarred tissue. Other existing software platforms for cardiac structural and functional analysis with CMR are, for instance, Segment CMR and CAAS MRV. Segment CMR is produced by Medviso and it offers LV analysis by machine learning [54]. CAAS MRV is produced by Pie Medical Imaging and it produces an automatic generated 3D segmentation of the heart and automatic infarct detection [55].

3.3. CMR market

CMR imaging market is expected to grow in the upcoming years due to the increasing number of cardiovascular diseases and the need to appeal to non-invasive image techniques to study the patient's pathology.

Regarding its application, the market can be divided into hospitals, which mainly dominated this market in 2018 and it is expected to keep its position. Secondly, diagnostic laboratories and research institutions are also markets interested in cardiac MRI.

Major players that operate in the CMR market are the following:

- General Electric Company
- Philips Healthcare
- Medtronic
- Canon Medical

Regarding imaging softwares, Siemens Healthineers in 2018 announced a collaboration with Circle Cardiovascular Imaging to develop with respect to MRI scanner application products and post-processing tools in order to improve CMR imaging diagnostic tools and increase accessibility of CMR. Moreover, they agreed to allow users to use cmr42 on Syngo.via, an integrated imaging software for multimodelling and allows connection to Siemens Healthineers Digital Ecosystem Store, thus, allowing a tight integration between them, improving diagnostic capabilities of CMR images and digitalizing healthcare.

3.4. Future perspective of the market

There are different research groups and non-profit organizations dedicated to improving cardiac health by investigating them and spread awareness over the population with the purpose of impulse population initiative to care more about their health. It is being achieved by impulsing cardiopathology awareness, CPR seminars, etc. The combination of these approaches are presenting significant changes and its investing will induce improvements in the future.

There is a considerable rise in cardiac diseases in the population so, both imaging softwares and CMR scans have started to develop a tendency in order to emerge in a wide scale. In addition, constant changes in the regulatory and legal matter concern the rise of rivalry and competition between companies. For this reason, it is believed that cardiology market will keep arising and achieve a more important role in the future, especially considering the impact of biomedical engineering and multidisciplinary professions involving health and technology, which help to implement new technologies for treatment and diagnosis techniques, especially regarding image related tools.

However, in the clinical practice it is needed to work in the standardization of the use of MR methods in cardiac applications since there is a large range of options with different accuracy and regional bias.

4. CONCEPTION ENGINEERING

In this section, some possible solutions regarding different aspects for the development of this project will be exposed in order to choose a proper method for it. First, the different options of medical images in which perform the LVWT assessment will be discussed. Then, knowing which type of medical image will be used for the purpose of this project, the segmentation software will be selected in basis of the features that the software offers regarding the study of this type of image. Finally, the statistical environment in which the analysis of the results will performed will also be studied to select a proper software.

4.1. Study of solutions

4.1.1. Type of medical image

- **Thoracic CT**

A CT scan is a X-ray imaging technique in which a beam of X-ray are focused on the body as they rotate around it. It can show smaller structures in different plans (see *Figure 19*). This technique offers enough spatial resolution to provide detailed anatomical information about the myocardium, coronary arteries and pericardium. In addition, a reconstruction in 3D can be performed.

This type of images can be enhanced, for instance, with iodinated contrast agents to highlight the lumen of the coronary arteries. Thus, CT in ischemic cardiomyopathy with LV myocardial infraction can show focal ventricular wall thinning, calcified replacement of myocardium and aneurysms [6]. In addition, it can assess ventricular function, myocardial hypertrophy and dilated cardiomyopathy. CT images can assess cardiac masses to their size and density, but they cannot assess qualitatively tumours or morphologically variated structures and they cannot provide flow information [56].

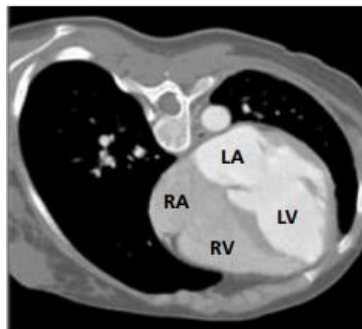


Figure 19: Transaxial CT image showing the left atrium, right atrium, right ventricle and left ventricle [56]

- **LGE-CMR**

As mentioned in this project, MRI present tissue information. MRI is commonly used to study and visualize soft tissues or organs since in this type of images, bones do not obscure them. It characterises injuries, tumours, inflammatory diseases, degenerative joint problems, etc... and it is widely used to evaluate organs of the chest and abdomen, including the heart.

This image technique does not involve ionizing radiation since it is based on imaging nuclear magnetic resonance signal mainly from the hydrogen nuclei, which consists of measuring the relaxation time at which the protons return to their random orientation of magnetic moments after an external magnetic field is applied and then removed in order to characterize the tissue composition.

In addition, it provides high tissue contrast resolution, high-resolution imaging and a 3D reconstruction can be performed. However, the time needed to acquire an MRI image is higher than in CT scans. For this technique, different pulse sequences can be used to highlight differences in signal of various soft tissues. As commented, two common pulse sequences used for this technique are T2-weighted sequence and T1-weighted sequence, which is commonly considered during the study anatomic structures and, combined with gadolinium, it can assess scarred tissue [57].

4.1.2. Segmentation softwares

- **ADAS 3D**

ADAS 3D (which stands for Automatic Detection of Arrhythmic Substrate) is a post-processing imaging platform that offers interventional procedures planning and guidance to support clinical decisions. It is developed in partnership with Hospital Clínic de Barcelona and it is being evaluated clinically in collaboration with important hospitals around Europe and America. It converts CMR and CT images into visual 3D images in order to identify the CC before the performing the procedure. Using cardiac DICOM images, it offers post-processing modules for the LV and the left atrium that identify fibrosis and enable viewing surround anatomical structures to the ventricle or atrium [58]. *Table 2* resumes its important features and *Figure 20* shows its interface.

Anatomical structures	LV and left atrium (LA)
Segmentation	Semi-automatic (10-15min)
Segments	AHA
LV features	Interactive 3D view of the LV and its characteristics Fibrosis visualization in 3D-coloured images Scar and BZ border quantification LV wall division in 9 layers from endocardium to epicardium Visualization autodetected CC LVWT quantification Visualization of other adjacent anatomical structures Scar segmentation can be manually adjusted 3D images and relevant myocardial information exportation to files in formats accepted by EP navigation systems. Data exportation from the EP navigation system to use it to compare MRI information to electro-anatomical data.

Table 2: Resume of ADAS 3D relevant information [58] [59]

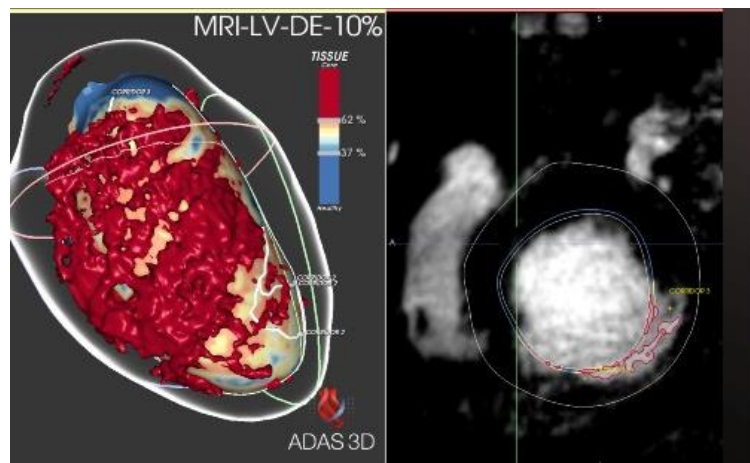


Figure 20: Screen shot of ADAS 3D LV showing a CC in white, scar core volume in red, BZ in orange and healthy tissue in blue in the 10% layer of the LV (the most endocardial layer) and the correspondence between a point in the 3D view and its position in the MRI [58]

- **Segment CMR – MEDVISO**

Segment CMR is a software used for CMR images analysis and it is the only clinically approved software on the cardiac market to include feature tracking and tagging analysis in one package. It is available for researchers and clinicals and it is developed with the collaboration with Lund Cardiac MR Group at Lund University and Skåne University Hospital in order to develop the best tools for image analysis for both clinical and research purposes [60]. *Table 3* resumes its features and *Figure 21* represents its interface.

Anatomical structures	LV and right ventricle (RV)
Segmentation	Semi-automatic / Artificial intelligence-based / manual
Segments	AHA
Features	LV analysis by machine learning algorithms RV analysis by automatic and semi-automatic tools Fully automated scar segmentation and quantification, validated and applicable to images from all vendors. Strain analysis for both LV and RV Flow analysis Perfusion analysis Signal intensity analysis for ROIs Imbedded patient database with commenting feature Scar segmentation can be manually adjusted

Table 3: Resume of Segment CMR relevant information [60]

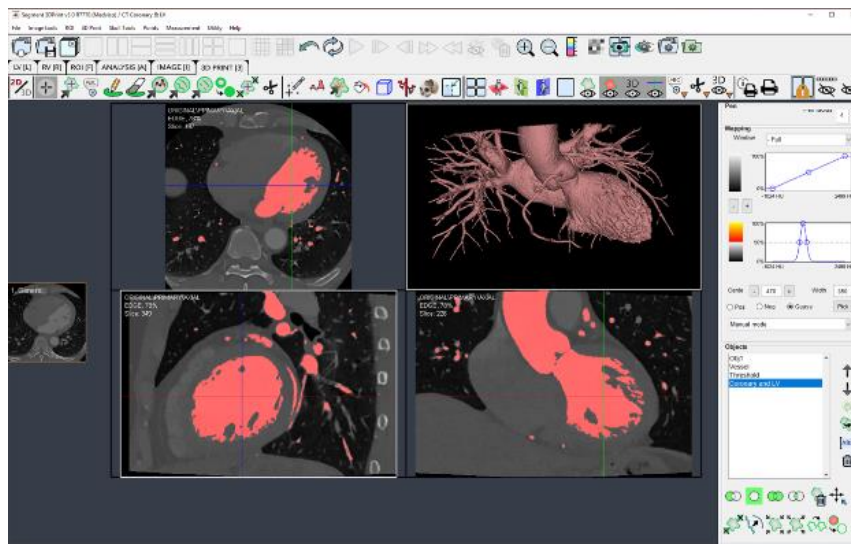


Figure 21: Example of Segment CMR interface [60]

4.1.3. Statistical analysis softwares

- **SPSS Statistics**

This software used mostly for hypothesis testing, predictive analysis or solving business problems that offers tools for advanced statistical procedures for statistical studies, including data registration in a data base, linear regression and visual graphing. It also allows to define the name, type and label and more features of different variables [61].

Some of the features that it provides are exposed below:

- Descriptive statistics: summarization and standardization of scale variables using descriptive procedures. It studies relationships between scale and categorical variables. It is useful to obtain summary comparisons and normally distributed scales variables in order to identify unusual cases across some variables computing z scores.

- Prediction models: availability to model the value of a dependent variable based on its relationship with predictor variables using linear or ordinary least square regression.
- Data preparation: it identifies unusual cases and invalid cases, variables and data values and it prepares data for modelling. Thus, it avoids data entry errors, which is important in cases where data collection is large.
- Correlations: this software measures how variables are related to each other by using bivariate correlations, partial correlation or other types of procedures.
- Classification
- ANOVA, one sample, paired sample and independent sample T-Test
- Bootstrapping
- Graphs and charts
- Output options

- **Microsoft Excel**

Excel is a common and widely used program for managing data sets. It presents some statistical capabilities to perform statistical calculations that do not require specialized data analysis model nor present a huge data set since these capabilities are limited, so it does not allow to perform advanced statistical analyses. Some tests that can be performed in Excel Statistical Analysis are the following:

- Descriptive statistics
- ANOVA
- Sampling
- Regression
- Rank and Percentile

However, other common tests such as Paired T-test or Two-sample T-test can be performed manually with excel but they require several data arrangements.

- **RStudio**

R is a programming language that is widely used by researchers for statistical computing, analysis and graphing. It is a free software that requires programming code. Different packages can be used to performing statistical analysis depending on the type of tests needed for the statistical approach. Therefore, it can perform all the descriptive analysis, ANOVA, regression equations... Its interface also offers the option to visualize and modify data, identify important rows or columns. Moreover, plots can also be done with R, which is commonly used in data science [62].

4.2. Proposed solutions

In the previous section, different alternatives for the development of this project have been presented and studied. Now, it will be exposed the chosen options for the proper development of this project.

To begin with, it has been chosen to study CMR images to perform this project due to their ability to offer myocardial tissue characterization, crucial for this project, and thus, scarred tissue information and CC detection, which later, combined with the LVWT study, the performance of this project will be more comfortable because the study will be performed using the same images for CC detection and LVWT assessment. Also, the fact that the previous study, in which this project is based, used CMR images, also conditioned this election because it is desirable to study the same images in order to work with the same parameters used to assess the tissue characterization threshold, which determines the value of the variables used for this study and the CC detected and, therefore, the arrhythmogenic CC of the patient.

Then, the segmentation software chosen was ADAS 3D Medical since it offers particular tools regarding the myocardial characterization and CC detection in CMR images and the LV visualization. The main important feature is the LVWT study, which allows to obtain the mean value of the WT in every AHA-segment, the conventional LV segmentation model, so it will be widely easy to interpret, and a very illustrative and organized way to represent every CC, which is useful in order to determine clearly the segments affected by the CC and differentiate different CC in a single patient. In addition, this software is suitable to this project because it offers layer-based detection to detect transmural CC, useful to evaluate the effect of the wall thickness involving the CC after the ablation since it offers information about the range of the CC.

Furthermore, it allows to modify the threshold used to characterize the myocardium, which is a very appropriate tool to use in cases in which the CMR was not acquired in the exact proper time and the image resulting shows different highlighting for the scarred tissue. Thus, the threshold needed must be adjusted depending on the degree of earliness or lateness of the LGE-CMR acquisition. The interface of this software also allows an easy interaction and comprehension of the software's workflow and segmentation. In addition, this software is developed in collaboration with the Arrhythmia's Unit of the Hospital Clínic de Barcelona and they are both in continuous contact to communicate and solve problems or needs that the electrophysiologists may encounter regarding the post-processed images. Thus, it will be easier to interact with the software's developers.

Finally, the software chosen for the statistical analysis was SPSS Statistical. Even though Excel and R are helpful softwares for data organization and analysis, using a statistical and specially developed analysis software like SPSS can offer more accurate results and data analysis with an interface that allows an easier way to work with the data base and to perform the statistical study.

5. DETAILED ENGINEERING

5.1. Data

The data used on this study consists of CC and WT information extracted from the same patients used in the study in which this project is based. In *Table 4*, the characteristics of the patients used for this project are presented.

Baseline characteristics	Total population (n=26)
Age (years)	63.8 ± 12.3
Male gender	96.80%
Ischemic cardiomyopathy	74.20%
Smoker	16.10%
Hypertension	64.50%
Diabetes	54.80%
Dyslipidemia	64.50%
LVEF	36.1 ± 10.7
Beta-blocker therapy	54.80%
Amiodarone therapy	64.50%

Table 4: Summary of the patients used for this study

Regarding the patients used to study the correlation between the outcome of the catheter ablation and the wall thickness affected by the CC, since the availability of image information after the ablation from these patients was limited, only 10 of the patients above could be studied because the rest did not present accessible post-procedural image.

5.2. Methodology

The methodology followed for the practical part consisted in the next steps:

First, a data base with information assessed in the previous study, such as arrhythmogenicity, maximum length, width and protectiveness, for every CC in every patient was used. From this information, the arrhythmogenicity was the main data needed for this project, which was already assessed in the previous study by studying the activation map (see *Figure 3*) in every patient in order to detect the main CC that triggers the tachycardia.

Then, starting from this data base, it was registered for each CC which AHA segments were affected by the CC and which segments were not. The wall thickness of every segment for every patient was also registered, as well as the AHA segments affected by CC that some patients presented after the catheter ablation.

As exposed, the software used to study the LGE-CMR images is ADAS 3D. Here are presented the steps and tools used to perform both LV and Wall-thickness study. To begin with, when a case is open with this software, the CMR and CT attached to the case are shown.

For every type of image attached to the case, different studies can be applied. In *Figure 22* it can be seen one case that presents two types of images acquired (DE-MRI and CT). The type of analysis that can be studied for DE-MRI are resumed in *Figure 23*.



Figure 22: Principal screen of ADAS 3D software [59]

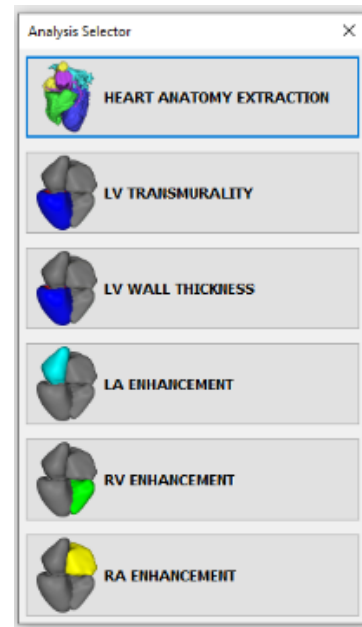


Figure 23: Analysis selector [59]

Hence, LV Enhancement and LV Wall thickness are the only analysis of interest for this project and here are presented the steps followed in order to obtain the information needed for the study:

- **LV ENHANCEMENT**

The first step for this analysis is the **segmentation** of the patient's cardiac model. It consists of placing 4 landmarks on any of the three planes of the CMR image (since the planes are synchronized). These landmarks are the centre of the aortic ring, the centre of the mitral ring, the epicardial side of the apex and the centre of the tricuspid ring and they can be seen in *Figure 24*.

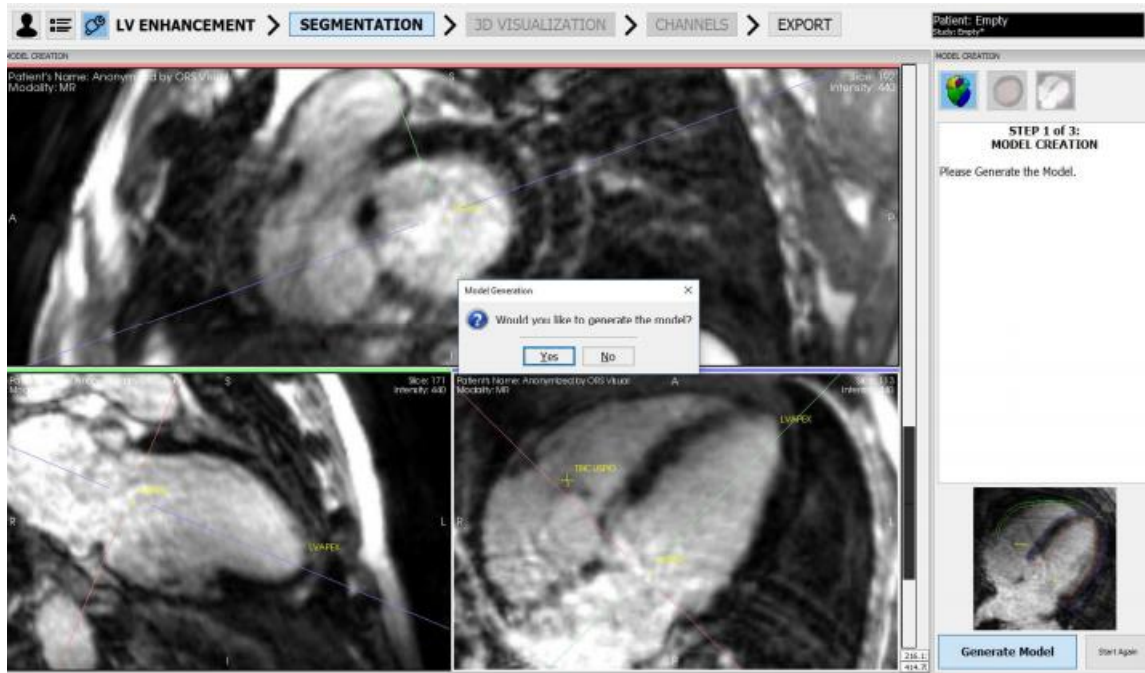


Figure 24: First step of CMR LV segmentation, consisting on start generating the model by using four landmarks [59]

Consequently, cardiac model can be adjusted by drawing the endo and epicardial contours, which can be seen in red and blue, respectively, in basal, mid and apical short axis slices seen in red, green and blue, respectively in the right bottom image in Figure 25.

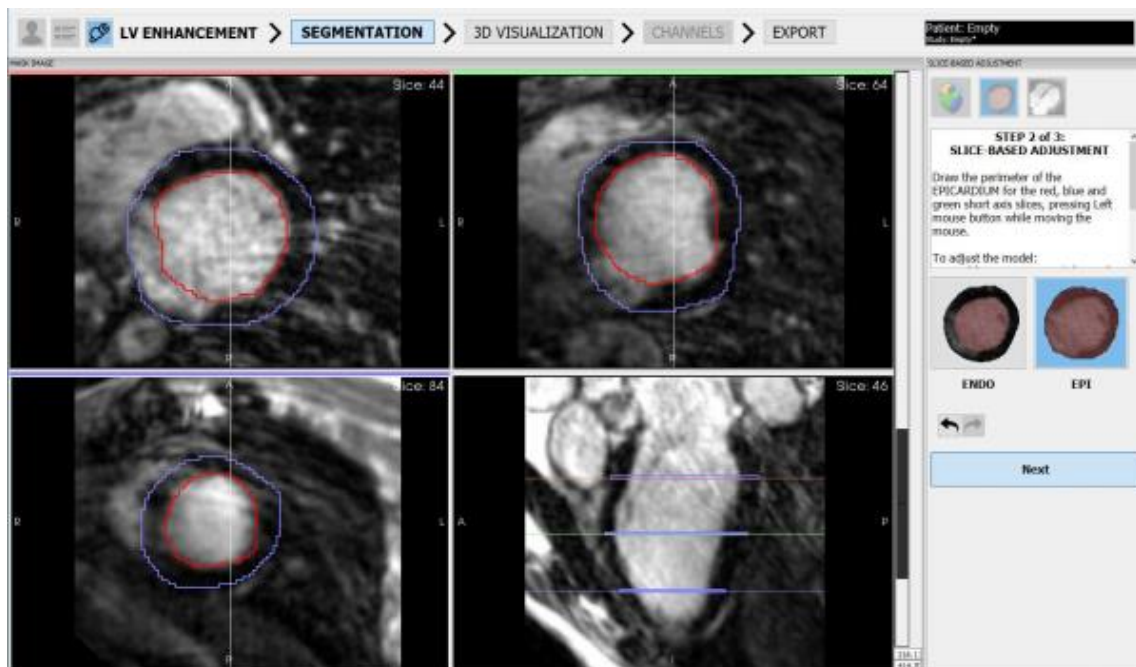


Figure 25: Screenshot of the second step for segmentation, slice-based adjustment, in ADAS 3D [59]

Finally, the provisional model that this software computes using the landmarks and endocardial and epicardial contours previously defined has to be adjusted to obtain an accurate threedimensional representation by modifying independently or simultaneously these contours in all the planes, as it can be seen in *Figure 26*. In addition, the subjacent anatomical structures can also be adjusted.

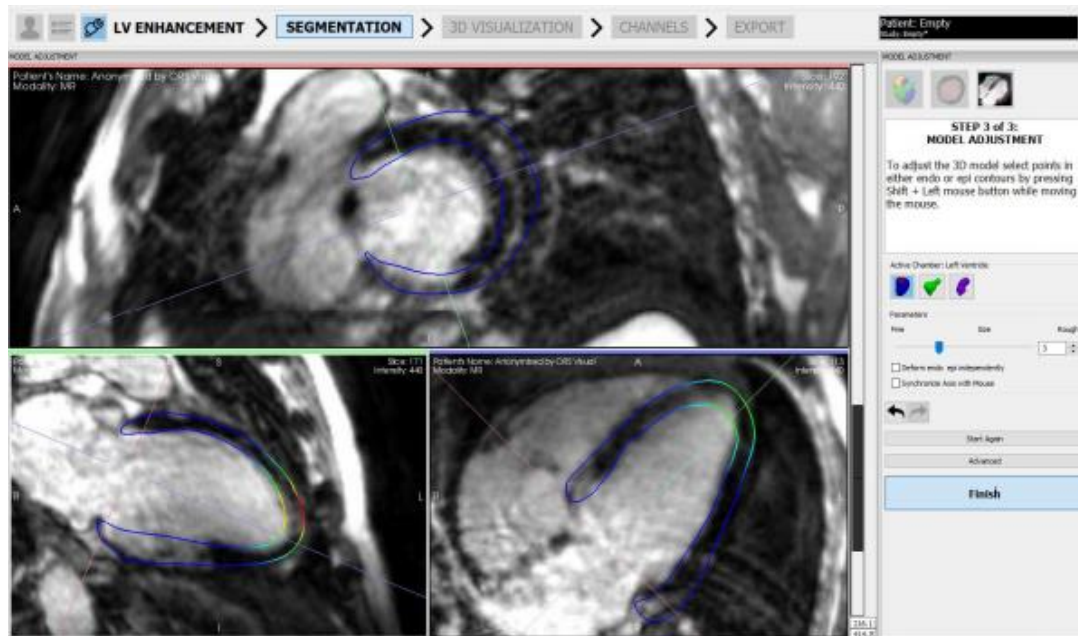


Figure 26: Screenshot of the third step for segmentation, model adjustment, in ADAS 3D [59]

Secondly, the **3D visualization** step allows to specify the tissue characterization threshold and visualize the LV and the scarred tissue, the BZ and the healthy tissue, as seen in *Figure 27*. In this figure, some features are highlighted and explained above:

1. Here it is represented the layer in which the LV is being visualized, 10% represents the most endocardial layer and 90% represents the most epicardial layer.
2. This colour bar allows to change the threshold used for the tissue characterization. In this case, the thresholds are settled at 65-35%. The colour map represents in red the scarred tissue and in blue the healthy tissue. The BZ is represented according to its potential contribution to slow conduction zones in different degradation colour between red and blue (see *Figure 27*).
3. In addition, the threshold can be changed by writing manually the threshold using these sliders on the right.
4. Here, the orientation of the LV representation in every moment is represented with a mannequin.

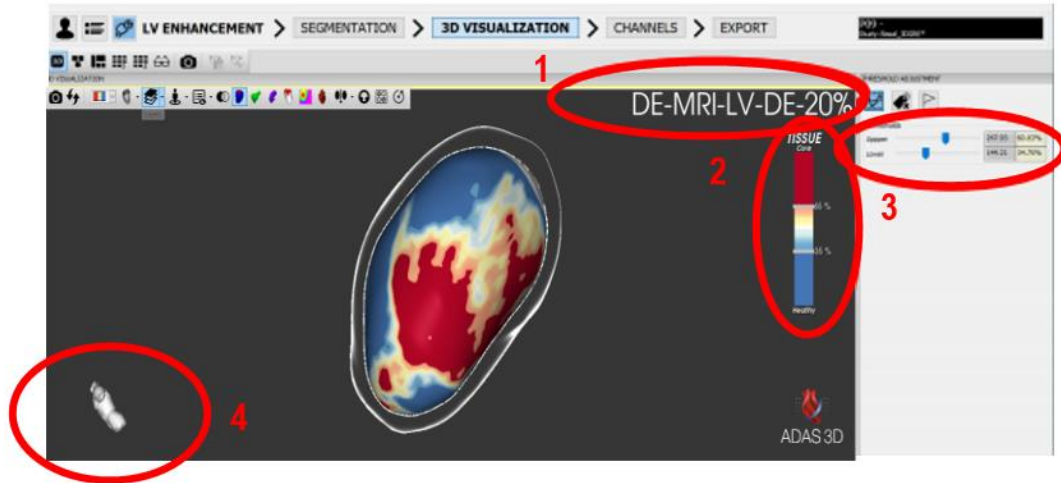


Figure 27: Representation of the 3D visualization and features in ADAS 3D interface characterising the LV myocardial and showing the healthy tissue (in blue) and the scarred tissue (in red). Screenshot taken by the author of this document

The next step automatically computes the CC, which in this software may be called corridors or channels. It uses a specified threshold to set the minimum length to consider that a specific corridor of BZ tissue can be considered as an actual CC. In addition, particular CC can be removed or added manually from the list of automatically detected CC under clinical considerations. In *Figure 28* it can be seen one of the two CC that a patient represents and the corresponding AHA segments affected by it (segments 7, 8, 13 and 14).



Figure 28: Representation of one CC visualization and the AHA segments. Screenshot taken for the author of this document

In addition, some other features such as the representation of the subjacent anatomical structures (aorta and right ventricle), the visualization of the core in 3D (see *Figure 29*) and exportation of the processed data can also be useful.

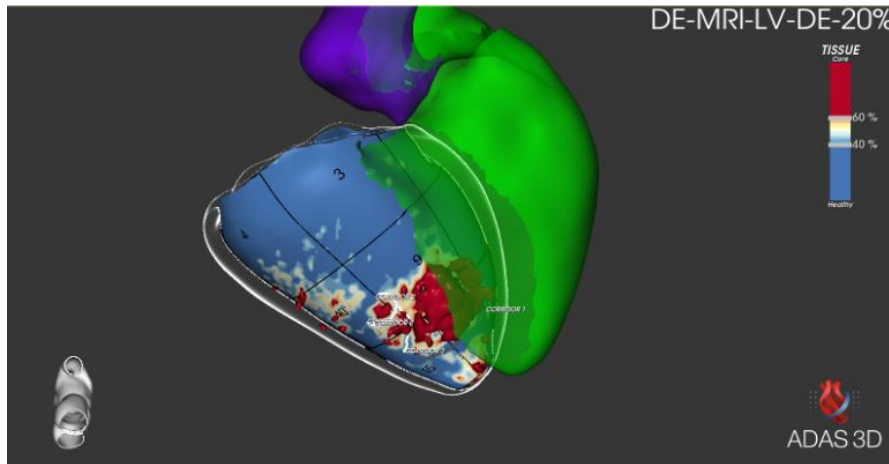


Figure 29: Representation of the LV, CC, AHA segments, core tissue in LV, RV and aorta in ADAS 3D. Screenshot taken by the author of this document

Hence, using this AHA segments and CC visualization and for each CC from the 26 patients, for each segment it was registered if it was affected by a CC or not.

- **LV WALL THICKNESS**

The second study needed was the LV wall thickness. The interface and process for this analysis is very similar to the previous one explained but the CC cannot be visualized. However, AHA segments can also be represented in this study (see *Figure 30*) and, using the statistical analysis tool offered by this software, the minimum, maximum and mean thickness of every segment is computed (see *Figure 31*). Moreover, the software represents in a scale of colours the thickness, showing in blue the thicker regions and showing in orange the thinner regions.

As beforementioned, LVWT is computed automatically measuring the distance between the endocardial and epicardial contour defined manually in the segmentation step. Thus, it relies strongly on a manual step that can be affected by user variability. In addition, this software does not allow to observe two cases or two different studies at the same time so first, the information about the segments affected by CC were registered and then, using the LVWT study, the wall thickness of every segment were registered.

This methodology was performed for every CC of every patient.

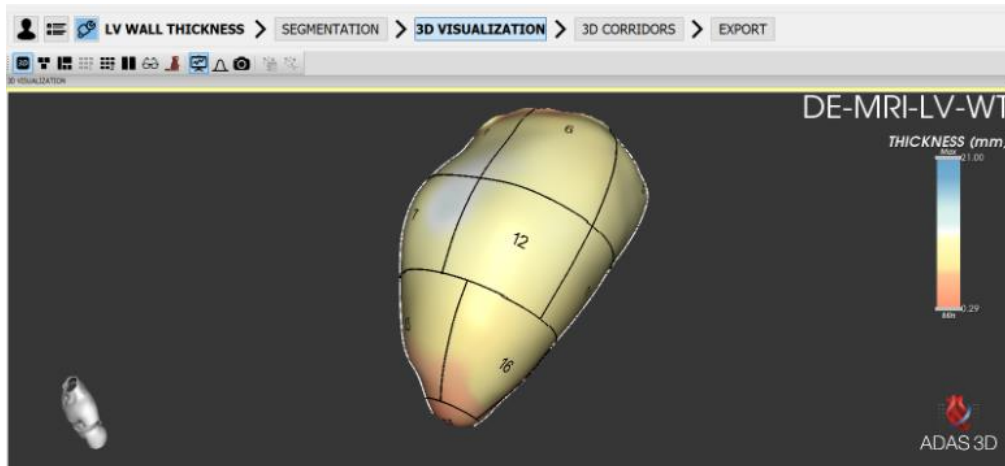


Figure 30: Illustration of the LV Wall Thickness representing in blue the thicker areas and in orange the thinner areas. The corresponding AHA segments are also shown by ADAS 3D. Screenshot taken by the author of this document

VT Grid Viewer

Numeric Data

SEGMENTATION-CT	Numerical	Layer Tissue	Image Tissue	Layer 17 AHA Numerical	Layer 17 AHA Tissue
Name	Min	Max	Mean	SD	
1 Layers AHA	0.29	2.1	6.39	1.66	
2 LVWT AHA Segment 1	2.6	13.5	6.07	1.68	
3 LVWT AHA Segment 2	0.91	2.1	6.93	1.65	
4 LVWT AHA Segment 3	3.07	7.04	4.92	0.84	
5 LVWT AHA Segment 4	3.55	8.17	5.5	0.68	
6 LVWT AHA Segment 5	2.94	9.25	6.75	1.51	

Figure 31: Numeric data representation of the minimum, maximum, mean and standard deviation LV Wall Thickness values of every segment. Screenshot taken by the author of this document

Thus, the mean value of every segment from every patient was registered in the data base.

Since the heterogeneity of the LV can change after the catheter ablation procedure due to the formation of new scarred tissue, some patients could present no CC and for some patients the software could still present some CC, but they may not be pathological nor the same from the CC detected before the procedure. For this reason, for the patients used to study the outcome of the procedure, the data about the presence of CC in the segments was registered for patient and not for individual CC.

5.3. Results

Since the statistical study consists on comparing means from two independent groups (LVWT of arrhythmogenic CC and LVWT of non-arrhythmogenic CC) and study its significance, a T-test was performed for both arrhythmogenicity and ablation outcome study. *Table 5* resumes the relevant results for the arrhythmogenicity study. From the 26 patients' data available for this project, a total amount of 79 CC were used for this study, for which 30 of them corresponded to arrhythmogenic CC and 49 corresponded to non-arrhythmogenic CC.

Total cases (CC)	Standard deviation	Difference in means	p-value	95% confidence interval	
				Inferior	Superior
79	0,59108	0,05832	0,922	-1,12215	1,23880

Table 5: Resume of relevant T-test results

The corresponding box plot of this study (Figure 32) was also computed, where 1 represents arrhythmic CC and 0 represents non-arrhythmic CC. As explained, the LV wall thickness has been computed using the mean value for every segment.

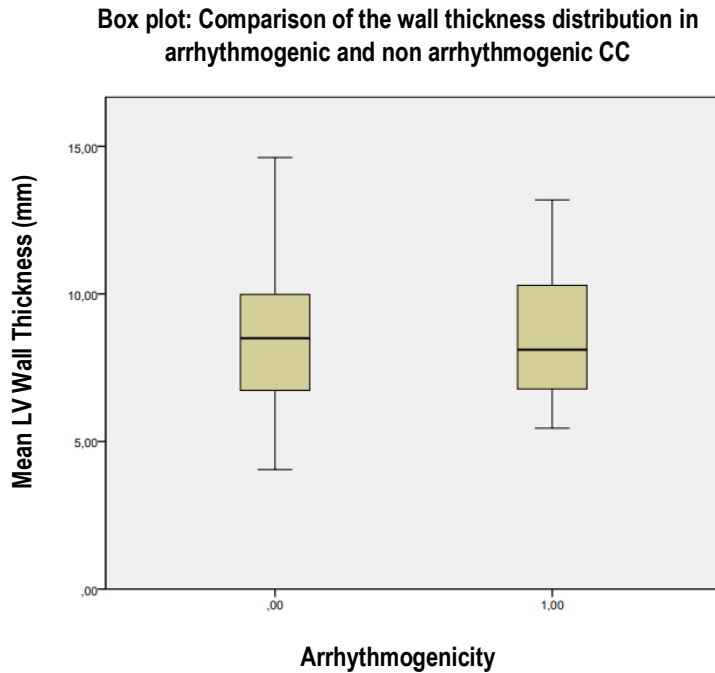


Figure 32: Comparison of the wall thickness distribution by type of CC in which 0 represents the non-arrhythmic CC and 1 represents the arrhythmic CC

In addition, a study of the distribution of both arrhythmic and non-arrhythmic CC among the 17 segments was computed (see Figure 33).

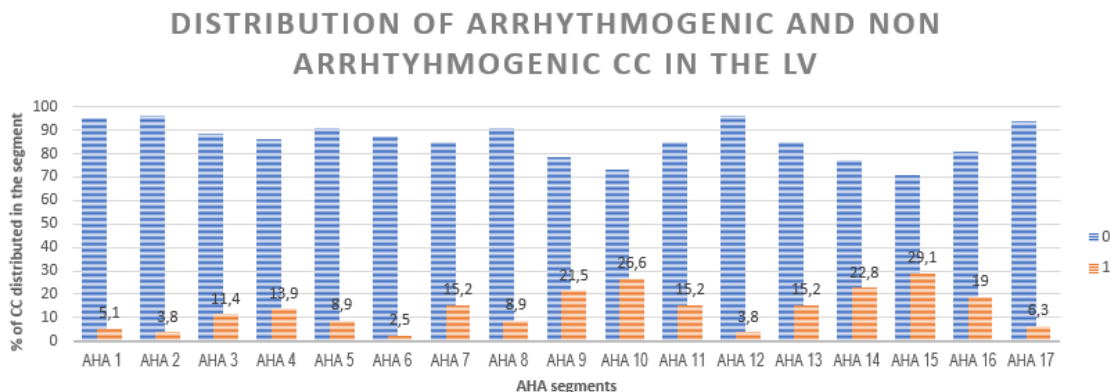


Figure 33: Distribution of the arrhythmic and non arrhythmic CC in the LV by segments, where 0 represents the non arrhythmic CC and 1 represents the arrhythmic CC

5.4. Discussion

To sum up the results presented, since the 95% confidence interval includes the value of 0, it includes the possibility that the difference between the mean LV wall thickness for the segments affected by arrhythmogenic CC and for the segments affected by not arrhythmogenic CC may be null. Therefore, it cannot be concluded that there exists a difference between these two types of CC regarding their wall thickness value, as it can be represented in *Figure 32*.

Consequently, the p-value obtained shows that the results achieved are not significant enough to consider that there is a difference between the wall thickness of arrhythmogenic CC and not arrhythmogenic CC. In addition, since the p-value obtained is larger than 0.05, it indicates that the null hypothesis, which consists in assuming that the wall thickness of a CC does not present difference according to its arrhythmogenicity, cannot be rejected. Thus, it has to be accepted that the arrhythmogenicity of a CC is not related to its wall-thickness, which might also be advantageous to be aware of with the purpose of focusing the arrhythmogenicity in other features and maybe reject the arrhythmogenicity of a CC using this information as a complement to other characterising features of arrhythmogenicity.

Nevertheless, it is important to highlight that this study was performed with a limited number of patients, which certainly contributed to the obtainment of a large p-value that forced to reject the hypothesis. This constraint could be solved by studying a larger number of patients and CC in order to achieve a more reliable result.

In addition, *Figure 33* showed an interesting distribution of both types of CC through the segments 9, 10, 14 and 15, containing between 20-30% of the 30 arrhythmogenic CC studied in this project, that contribute to the mid and apical inferoseptal region of the LV (*Figure 34 and 35* shows an example of this region), which corresponds to a part of the septum that borders the left and right ventricles, it contains the left bundle branch (see *12. Appendix*) and it contributes to the pumping function of the heart. For this reason, this result could be interesting to investigate in the future including more patients and, hence, more CC to study and to assess a possible relationship between the arrhythmogenicity and a potential alteration or attribute of this region.

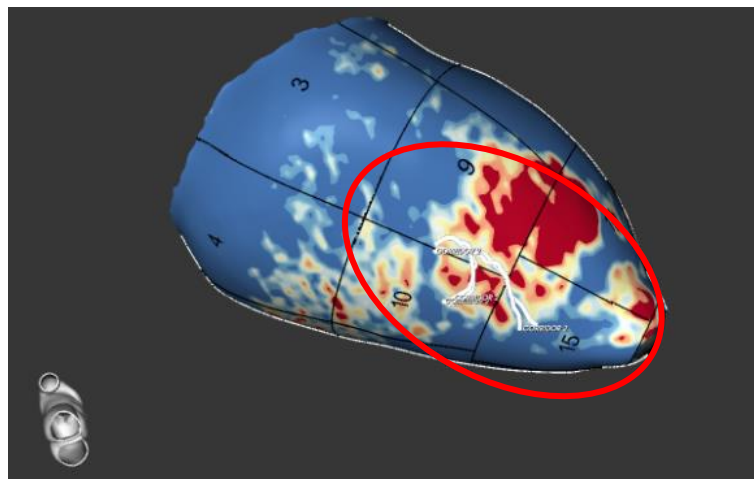


Figure 34: Inferoseptal region of the left ventricle containing one CC. Screenshot taken from the author of this document.

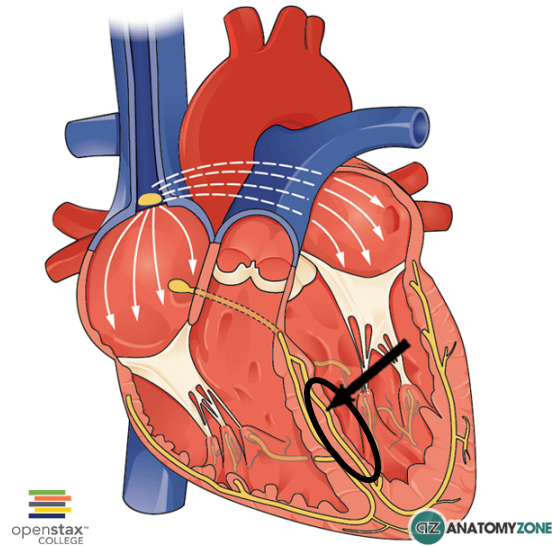


Figure 35: Representation of the inferoseptal region of the LV in a 4 heart chambers view [63]

Finally, regarding the study between the ablation outcome and the LV wall thickness, a further study could not be computed since the p-value obtained was extremely large and it has not been able to assess a tendency of CC distribution depending on the LVWT after the process.

6. EXECUTION CHRONOGRAM

In this section, the temporal organization of the different tasks performed during this project is explained. Moreover, a chronogram that represents these tasks graphically is presented in this section in order to offer a clear comprehension of the tasks and timings that have been followed to achieve the accomplishment of this project.

It is also important to mention that some tasks have extended their timings due to incidentals, which is explained in the following section.

6.1. Definition of tasks and timing

The tasks and their respective timings for the development of this project are presented and explained below:

- A. Bibliographic research about LVWT and AHA segments:** to begin with, a knowledge of the AHA segments was necessary to acquire in order to understand the conventional and accepted distribution of the LV and the assessment of the LVWT.
- B. Familiarization understanding with “Wall-thickness study” tool:** some period before starting the project was dedicated to acquiring knowledge about the ADAS 3D feature that allows to obtain statistical information about the LVWT in every AHA segment and to understanding how to interpretate this information. This task was performed at the end of the internship and it implied almost two weeks.
- C. Verification of the concordance between the patients’ LV data provided by the previous study and the patients’ files used for the WT study:** before obtaining the interested data about the patients’ CC, a verification that data of the patients used for the previous study and the data available for this project coincided was essential in order to establish a correlation between the results obtained from the previous study and the results obtained in this project. For this reason, data regarding the LV of each patient’s CC (such as arrhythmogenicity, length, mass, layers and AHA segments involved and protectiveness) provided by the previous study had to coincide with the data provided by the patient’s file used in this project in order to assure that the study is performed with the same files and, thus, the same data of the CC. This is due to the fact that some files may present changed variables that alter the information interested so it is important to make sure that the study is performed with the exact same data used for the previous study so that the result does not seem altered. This task lasted much of the project because some files were lost during the project and it was not possible to access to them nor work with their data unless it corresponded to the correct file until weeks later. However, part of the study was finished before the temporary loss of the files so some files were not affected by it.
- D. Registration of the data interested from each CC of each patient:** once the proper files of each patient was set, for each CC and for each of the 17 AHA segments, the segments that were involved by the CC were indicated in the SPSS Statistics data base and so was the value of the WT of every AHA segment. This task relied on the previous task, but it has been accomplished as the files were available. In addition, some files were obtained and verified from other sources in the meantime.
- E. Arrangement of the post ablation patients and their respective files:** postprocedural data was not available for every patient used for the first part of the study so an effort to

reach the maximum number of postprocedural patients files for the study was needed in order to find more patients and to the second part of the study. This stage lasted only for a few days since the number of patients available was limited.

- F. Registration of the post procedure information from each CC of each patient available:** once the available data was settled, from every postprocedural patient it was important to register the number of CC detected after the ablation and, for each of the 17 AHA segments, register which segments are still affected by the CC. This task lasted almost five weeks. However, it could have lasted less but in some files, wall-thickness study or AHA segments features did not run so a technical support provided by the software company was needed.
- G. Last verification of the new data registered, the data from the previous study and the files used for each patient:** before the statistical analysis, and extra verification of the data registered, and the files used for each patient was performed to assure concordance with the previous study, which lasted two weeks.
- H. Statistical analysis:** this step was performed with *SPSS software* and consisted on obtaining the results.
- I. Information extraction from the statistical results:** in this step the results were interpreted.
- J. Assessment of the relation between WT and the arrhythmogenicity and the ablation's outcome and discussion of the results:** this step consisted in understanding the results obtained and taking out the corresponding discussions.
- K. Writing of the memory of the final degree project:** it has been elaborated the memory for this project along with the practical part described above from February to June.

6.2. GANTT diagram

Table 6 represents the tasks explained in the previous section and the approximate timing task of each step of the project.

Task	Start	Finish	Duration (days)
A	16/11/2020	09/21/2020	18
B	12/03/2020	21/12/2020	13
C	21/12/2020	14/05/2021	105
D	20/20/2021	14/05/2021	74
E	28/02/2021	26/02/2021	7
F	26/02/2021	22/04/2021	40
G	07/05/2021	28/05/2021	16
H	28/05/2021	01/06/2021	3
I	02/06/2021	04/06/2021	3
J	07/05/2021	10/05/2021	2
K	10/02/2021	13/06/2021	88

Table 6: Project tasks with the corresponding duration

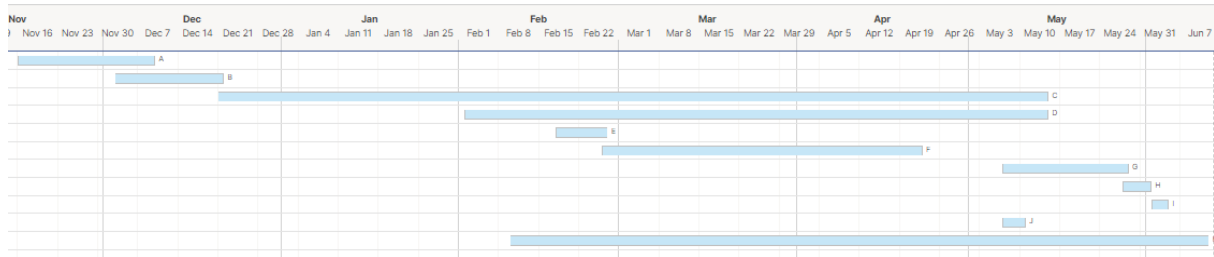


Figure 36: GANTT diagram of the project

Figure 36 represents the GANTT diagram, which represents the tasks and timings explained in the previous section. It can be seen that some tasks were performed simultaneously since they did not rely on each other and since the project was performed by one single student,

7. TECHNICAL FEASIBILITY

In this section, the internal factors of this project (which are its strengths and weaknesses) and the external factors (threats and opportunities) have been studied with a SWOT analysis.

7.1. Strengths

Considering that the purpose of this project is to continue and expand the range of a previous research by studying an additional variable to characterize the arrhythmogenic CC, the LGE-CMR scans are already performed in the hospital and the data regarding the arrhythmogenicity of all the CC is already assessed, as mentioned before. In addition, some aspects such as the patient's anonymization were already settled.

In addition, CMR images offer several advantages over other techniques, for instance no ionising radiation, reliable tissue characterization and improves image quality.

Moreover, it is important to consider the important commitment that presents the location in which this project is developed, which is the ICCV of the Hospital Clínic de Barcelona. It consists of a multidisciplinary research group that is committed with the implementation of non-invasive image techniques in order to approach an accurate treatment for patients with cardiopathologies and to evaluate, to study and innovate therapies performed nowadays in order to personalize and improve their outcomes. Thus, the background and the constant training and dedication for evolving that this location owns has been helpful to develop this project and solve doubts and issues.

7.2. Weaknesses

Nevertheless, this project also presented some limitations, for instance the number of patients available for this study. As beforementioned, this study used 26 patients to study the influence of the WT with the arrhythmogenicity of the CC and only 10 of these patients were studied to assess the influence of the WT with the outcome of the ablation, which would have been desirable to work with more postprocedural patients but due to lack of data availability it was not possible.

In addition, since the main objective of the project is to assess the WT of the CC, but these values were estimated using the mean value of the WT of every segment, it is important to

consider that the values used will present variability since the WT may not be homogeneous in a segment and a CC only represents a small percentage of the whole segment.

User variability for segmentation is another important issue to consider since this process is the one that determines the LVWT and other information from the LV.

Although LGE-CMR is commonly used for cardiac scar characterization, this technique presents some limitations such as potential image artefacts in patients wearing cardiac implantable devices that are not compatible with MRI, long acquisition times, which conditions its application in patients that do not tolerate these circumstances.

7.3. Opportunities

It is known that the utility of imaging techniques such as cardiac MRI is the gold standard nowadays to evaluate and offer information of the patients' condition in a non-invasive way. Thus, for this project, the use of this techniques allowed the obtention of anatomy and functional information from the patients in order to characterize the myocardium and calculate the effect of the therapy performed to the patients, which is crucial for the development of this project.

In addition, as commented, the study of the LVWT is relatively new and this study can be promising since it can offer several benefits to the patients that suffer from VT as its information can help to acquire better interpretation of the patient's pathology and, therefore, perform a better approach and strategy for the catheter ablation. Thus, it can reduce the time dedicated to treat each patient and improve the outcome by providing the latest research tools adapted to clinical practice.

7.4. Threats

Several automatic segmentation algorithms have been studied and proposed for solving user variability and offer accurate cardiac segmentation but they are still not validated and their applications in clinical environment is challenging due to patient variability. In addition, large data sets are necessary in order to train and evaluate these algorithms, which sometimes may not be available.

In addition, several regulations and directives regarding patients' safety during image acquisition, and the requirement of their consent for the procedure and the use of their information for clinical and research purposes represent a restrictive factor for the development of this type of study.

Finally, *Table 7* represents the SWOT analysis.

SWOT ANALYSIS	
<i>Internal analysis</i>	<i>External analysis</i>
Strengths	Threats
<ul style="list-style-type: none"> - Continuation of a previous research - Research group with commitment 	<ul style="list-style-type: none"> - Automatic segmentation requirement - Healthcare regulations
Weaknesses	Opportunities
<ul style="list-style-type: none"> - Limited number of patients - Mean WT value and user variability - LGE-CMR limitations 	<ul style="list-style-type: none"> - Promising technology - Few LVWT studies

Table 7: SWOT analysis

8. ECONOMICAL FEASIBILITY

In this section the costs involved in this project is presented, including the costs of the software used, the CMR images used, payrolls and fungible products.

To begin with, it is assumed that a salary of a student is 17€/h. Since the amount of hours needed for this project is 300h, the cost ascends to 5.100€.

The MRI scans performed and used for this project were provided by Hospital Clínic de Barcelona.

Regarding the electricity that the computers consumed for this project, it has considered that for 280h of use and a consumption of 400W/h: $0,400\text{W/h} \cdot 280\text{h} \cdot 0,14968\text{€/kWh} = 16,46\text{€}$. One of the computers used is self-owned, which costed 230€, and the other one, which had access to the softwares needed for the project and the patients' data, was provided by Hospital Clínic de Barcelona since these procedures belong to routine clinical practice.

The software used during the development for this project was ADAS 3D, provided by Hospital Clínic de Barcelona as this program is developed in partnership with this hospital. For the statistical analysis, the software used was SPSS Statistics, a free statistical software platform developed by IBM and commonly used for researchers.

To sum up, in *Table 8* it is shown cost of every element used for this project and the total cost, which was 5.790,96€. It can be seen that the main costs of this project are dedicated to human resources.

Item	Cost (€)
Student	5.100
Electricity	16,46
MRI scans	0€ <i>(Provided by Hospital Clínic de Barcelona)</i>
T-jove travel card for 6 zones (x2 units)	444,50 (222,25€ per unit)
License	
ADAS 3D Medical SL	0€ <i>(Provided by Hospital Clínic de Barcelona)</i>
IBM® SPSS® Statistics	0€ <i>(Provided by Hospital Clínic de Barcelona)</i>
Devices	
Laptop	230€
Computer with access to ADAS 3D	0€ <i>(Provided by Hospital Clínic de Barcelona)</i>
Total	5.790,96€

Table 8: Resume of the total costs of this project

9. NORMATIVE AND LEGAL ASPECTS

This project has used real data from patients whose CMR images were acquired in the diagnostic centre of the hospital. All of them fulfilled and handed an informed consent about the catheter ablation intervention and both the electrophysiological study and MRI study.

It is important to mention that no compromised information from the patients was displayed in any moment since all the patients' data were previously anonymised and they were treated confidentially, following the Data Protection Act.

In addition, the patients fulfilled a consent regarding the use of their data for research and investigation purposes. The software used for the LV segmentations and CC detection, ADAS 3D Medical SL, has obtained the ISO certification with number MD 714518.

For this project, legal requirements for acquiring and using CMR images under the Spanish legislation, which involves the Directive 2013/35/EU regarding the regulation of the minimum safety standards regarding the exposure to electromagnetic fields, have been studied.

10. CONCLUSIONS

In conclusion, this project has highlighted the importance of imaging, specially before the catheter ablation procedure. In addition, as mentioned in this study, the importance of its role has been increasing over the last years since it has been demonstrated that obtaining myocardial tissue characterization information before the procedure allows to prepare a better approach for the ablation. In addition, CMR images are recognized as an essential imaging tool due to its reliability and safety. Therefore, it is important to offer easy systems to perform the previous study of the patient with LGE-CMR images and then, export and integrate these images to the navigation system during the procedure in order to perform the electrophysiological study with all the possible information from the beginning. Furthermore, its standardization and protocol set up is also important to compare studies and research performed from different centres.

In addition, it is important to comment the upcoming rise of the CMR softwares market to offer more features, more quality and more accessibility to the whole LV to the physicians and professionals dedicated to this field in cardiology. Hence, providing more resources and LV information for the electrophysiologists to perform a better approach of the procedure. Regarding segmentation techniques, it has become a interdisciplinary field that has grown over the years but further research in this field is still required to achieve more advances and automatization.

Regarding the results presented, the hypothesis proposed in the beginning of this project could not be demonstrated. The results showed poor significative differences between the LVWT values for arrhythmogenic CC and no arrhythmogenic CC. Specially, the study regarding the outcome of the ablation in relation to the LVWT of the AHA segments affected by the CC was not able to provide relevant information due to limited patient information used. Therefore, these results showed no correlation between the LVWT values depending on the type of CC nor between the outcome of the procedure depending on the LVWT values of the interested segments but since the p-value obtained was to large, further research using the necessary amount of patients to obtain a more reliable p-value would be interesting to propose in the future.

However, the results showed an interesting distribution of the arrhythmogenic CC through the segments that could be interesting to study in the future with more patients and more CC because it could offer information regarding the characterisation of arrhythmogenic CC regarding its location in the LV, useful for further research in this field.

To conclude, it is important to highlight the role of technology and biomedical engineering in this field since it has been demonstrated how CMR imaging relies on new and innovative techniques on pulse sequences to achieve an improved image acquisition, which is necessary to improve the diagnostical and therapeutical techniques offered to the patient in order to obtain better outcomes and more efficiency in the techniques that the patients need.

11. REFERENCES

- [1] Ludhwani D, Goyal A, Jagtap M. Ventricular Fibrillation. [Updated 2020 Aug 10]. In: StatPearls [Internet]. Treasure Island (FL): StatPearls Publishing; 2021 Jan-. Available from: <https://www.ncbi.nlm.nih.gov/books/NBK537120/>
- [2] Benito, B., & Josephson, M. E. (2012). Taquicardia ventricular en la enfermedad coronaria. *Revista Española De Cardiología*, 65(10), 939–955. <https://doi.org/10.1016/j.recesp.2012.03.027>
- [3] Batul, S. A., Olshansky, B., Fisher, J. D., & Gopinathannair, R. (2017). Recent advances in the management of ventricular tachyarrhythmias. *F1000Research*, 6, 1027. <https://doi.org/10.12688/f1000research.11202.1>
- [4] Mavrogeni, S., Petrou, E., Kolovou, G., Theodorakis, G., & Iliodromitis, E. (2013). Prediction of ventricular arrhythmias using cardiovascular magnetic resonance. *European Heart Journal - Cardiovascular Imaging*, 14(6), 518–525. <https://doi.org/10.1093/ehjci/ies302>
- [5] Andreu, D., Ortiz-Pérez, J. T., Fernández-Armenta, J., Guiu, E., Acosta, J., Prat-González, S., De Caralt, T. M., Perea, R. J., Garrido, C., Mont, L., Brugada, J., & Berruezo, A. (2015). 3D delayed-enhanced magnetic resonance sequences improve conducting channel delineation prior to ventricular tachycardia ablation. *EP Europace*, 17(6), 938–945. <https://doi.org/10.1093/europace/euu310>
- [6] Berruezo, A., Penela, D., Jáuregui, B., & Soto-Iglesias, D. (2021). The role of imaging in catheter ablation of ventricular arrhythmias. *Pacing and Clinical Electrophysiology*. <https://doi.org/10.1111/pace.14183>
- [7] Haqqani, H. M., & Callans, D. J. (2014). Ventricular Tachycardia in Coronary Artery Disease. *Cardiac Electrophysiology Clinics*, 6(3), 525–534. <https://doi.org/10.1016/j.ccep.2014.05.003>
- [8] Koplán, B. A., & Stevenson, W. G. (2009). Ventricular Tachycardia and Sudden Cardiac Death. *Mayo Clinic Proceedings*, 84(3), 289–297. <https://doi.org/10.4065/84.3.289>
- [9] Ary L. Goldberger, Zachary D. Goldberger, Alexei Shvilkin,. (2018). Chapter 21 - Sudden Cardiac Arrest and Sudden Cardiac Death Syndromes. In Z. D. Ary L. Goldberger, *Goldberger's Clinical Electrocardiography (Ninth Edition)* (pp. 217-225). Elseiver.
- [10] Samie, F. (2001). Mechanisms underlying ventricular tachycardia and its transition to ventricular fibrillation in the structurally normal heart. *Cardiovascular Research*, 50(2), 242–250. [https://doi.org/10.1016/s0008-6363\(00\)00289-3](https://doi.org/10.1016/s0008-6363(00)00289-3)
- [11] Gaztañaga, L., Marchlinski, F. E., & Betensky, B. P. (2012). Mecanismos de las arritmias cardiacas. *Revista Española De Cardiología*, 65(2), 174–185. <https://doi.org/10.1016/j.recesp.2011.09.018>
- [12] AlMahameed, S. T., & Ziv, O. (2019). Ventricular Arrhythmias. *Medical Clinics of North America*, 103(5), 881–895. <https://doi.org/10.1016/j.mcna.2019.05.008>
- [13] Benito, B., & Josephson, M. E. (2012). Ventricular Tachycardia in Coronary Artery Disease. *Revista Española De Cardiología (English Edition)*, 65(10), 939–955. <https://doi.org/10.1016/j.rec.2012.03.022>

- [14] Roberts-Thomson, K. C., Lau, D. H., & Sanders, P. (2011). The diagnosis and management of ventricular arrhythmias. *Nature Reviews Cardiology*, 8(6), 311–321. <https://doi.org/10.1038/nrcardio.2011.15>
- [15] Dukkipati, S. R., Koruth, J. S., Choudry, S., Miller, M. A., Whang, W., & Reddy, V. Y. (2017). Catheter Ablation of Ventricular Tachycardia in Structural Heart Disease. *Journal of the American College of Cardiology*, 70(23), 2924–2941. <https://doi.org/10.1016/j.jacc.2017.10.030>
- [16] Baez-Escudero, J. L., & Valderrabano, M. (2010). Ventricular Tachycardia. *Cardiology Secrets*, 261–265. <https://doi.org/10.1016/b978-032304525-4.00039-3>
- [17] Guandalini, G.S., Liang, J. J., & Marchlinski, F. E. (2019). Ventricular Tachycardia Ablation. *JACC: Clinical Electrophysiology*, 5(12), 1363-1386. <https://doi.org/10.1016/j.jacep.2019.09.015>
- [18] Andreu, D., Penela, D., Acosta, J., Fernández-Armenta, J., Perea, R., & Soto-Iglesias, D. et al. (2017). Cardiac magnetic resonance–aided scar dechanneling: Influence on acute and long-term outcomes. *Heart Rhythm*, 14(8), 1121-1128. <https://doi.org/10.1016/j.hrthm.2017.05.018>
- [19] Pohost, G. M. (2008). The History of Cardiovascular Magnetic Resonance. *JACC: Cardiovascular Imaging*, 1(5), 672–678. <https://doi.org/10.1016/j.jcmg.2008.07.009>
- [20] Ranjan, R., McGann, C. J., Jeong, E.-K., Hong, K., Kholmovski, E. G., Blauer, J., Wilson, B. D., Marrouche, N. F., & Kim, D. (2014). Wideband late gadolinium enhanced magnetic resonance imaging for imaging myocardial scar without image artefacts induced by implantable cardioverter-defibrillator: a feasibility study at 3 T. *Europace*, 17(3), 483–488. <https://doi.org/10.1093/europace/euu263>
- [21] Daire, J.-L., Jacob, J.-P., Hyacinthe, J.-N., Croisille, P., Montet-Abou, K., Richter, S., Botsikas, D., Lepetit-Coiffé, M., Morel, D., & Vallée, J.-P. (2008). Cine and tagged cardiovascular magnetic resonance imaging in normal rat at 1.5 T: a rest and stress study. *Journal of Cardiovascular Magnetic Resonance*, 10(1), 48. <https://doi.org/10.1186/1532-429x-10-48>
- [22] Lockie, T., Nagel, E., Redwood, S., & Plein, S. (2009). Use of Cardiovascular Magnetic Resonance Imaging in Acute Coronary Syndromes. *Circulation*, 119(12), 1671–1681. <https://doi.org/10.1161/circulationaha.108.816512>
- [23] Valbuena-López, S., Hinojar, R., & Puntmann, V. O. (2016). Resonancia magnética cardiovascular en la práctica cardiológica: una guía concisa para la adquisición de imágenes y la interpretación clínica. *Revista Española De Cardiología*, 69(2), 202–210. <https://doi.org/10.1016/j.recesp.2015.11.012>
- [24] Kramer, C. M., Barkhausen, J., Bucciarelli-Ducci, C., Flamm, S. D., Kim, R. J., & Nagel, E. (2020). Standardized cardiovascular magnetic resonance imaging (CMR) protocols: 2020 update. *Journal of Cardiovascular Magnetic Resonance*, 22(1). <https://doi.org/10.1186/s12968-020-00607-1>
- [25] Tseng, W. Y., Su, M. Y., & Tseng, Y. H. (2016). *Introduction to Cardiovascular Magnetic Resonance: Technical Principles and Clinical Applications*, *Acta Cardiologica Sinica*, 129–144. <https://doi.org/10.6515/acs20150616a>

- [26] Ripley, D. P., Musa, T. A., Dobson, L. E., Plein, S., & Greenwood, J. P. (2016). Cardiovascular magnetic resonance imaging: what the general cardiologist should know. *Heart*, 102(19), 1589–1603. <https://doi.org/10.1136/heartjnl-2015-307896>
- [27] Valbuena-López, S., Hinojar, R., & Puntmann, V. O. (2016). Cardiovascular Magnetic Resonance in Cardiology Practice: A Concise Guide to Image Acquisition and Clinical Interpretation. *Revista Española De Cardiología (English Edition)*, 69(2), 202–210. <https://doi.org/10.1016/j.rec.2015.11.011>
- [28] Hassan, S., Barrett, C. J., & Crossman, D. J. (2020). Imaging tools for assessment of myocardial fibrosis in humans: the need for greater detail. *Biophysical Reviews*, 12(4), 969–987. <https://doi.org/10.1007/s12551-020-00738-w>
- [29] Jo, Y., Kim, J., Park, C., Lee, J., Hur, J., & Yang, D. et al. (2019). Guideline for Cardiovascular Magnetic Resonance Imaging from the Korean Society of Cardiovascular Imaging—Part 1: Standardized Protocol. *Korean Journal Of Radiology*, 20(9), 1313. <https://doi.org/10.3348/kjr.2019.0398>
- [30] Bing, R., & Dweck, M. R. (2019). Myocardial fibrosis: why image, how to image and clinical implications. *Heart*, 105(23), 1832–1840. <https://doi.org/10.1136/heartjnl-2019-315560>
- [31] Caixal, G., Alarcón, F., Althoff, T., Nuñez-Garcia, M., Benito, E., & Borràs, R. et al. (2020). Accuracy of left atrial fibrosis detection with cardiac magnetic resonance: correlation of late gadolinium enhancement with endocardial voltage and conduction velocity. *EP Europace*, 23(3), 380-388. <https://doi.org/10.1093/europace/euaa313>
- [32] Roca-Luque, I., Van Breukelen, A., Alarcon, F., Garre, P., Tolosana, J. M., Borrás, R., Sanchez, P., Zaraket, F., Doltra, A., Ortiz-Perez, J. T., Prat-Gonzalez, S., Perea, R. J., Guasch, E., Arbelo, E., Berruezo, A., Sitges, M., Brugada, J., & Mont, L. (2020). Ventricular scar channel entrances identified by new wideband cardiac magnetic resonance sequence to guide ventricular tachycardia ablation in patients with cardiac defibrillators. *EP Europace*, 22(4), 598–606. <https://doi.org/10.1093/europace/euaa021>
- [33] Rashid, S., Rapacchi, S., Shivkumar, K., Plotnik, A., Finn, P. and Hu, P., 2015. Modified wideband 3D late gadolinium enhancement (LGE) MRI for patients with implantable cardiac devices. *Journal of Cardiovascular Magnetic Resonance*, 17(S1). <https://doi.org/10.1186/1532-429X-17-S1-Q26>
- [34] Peng, P., Lekadir, K., Gooya, A., Shao, L., Petersen, S., & Frangi, A. (2016). A review of heart chamber segmentation for structural and functional analysis using cardiac magnetic resonance imaging. *Magnetic Resonance Materials In Physics, Biology And Medicine*, 29(2), 155-195. <https://doi.org/10.1007/s10334-015-0521-4>
- [35] Zabihollahy, F., Rajan, S., & Ukwatta, E. (2020). Machine Learning-Based Segmentation of Left Ventricular Myocardial Fibrosis from Magnetic Resonance Imaging. *Current Cardiology Reports*, 22(8). <https://doi.org/10.1007/s11886-020-01321-1>
- [36] Karim, R., Bhagirath, P., Claus, P., James Housden, R., Chen, Z., Karimaghloo, Z., Sohn, H.-M., Lara Rodriguez, L., Vera, S., Albà, X., Hennemuth, A., Peitgen, H.-O., Arbel, T., González Ballester, M. A., Frangi, A. F., Götte, M., Razavi, R., Schaeffter, T., & Rhode, K. (2016). Evaluation of state-of-the-art segmentation algorithms for left ventricle infarct from late

Gadolinium enhancement MR images. *Medical Image Analysis*, 30, 95–107. <https://doi.org/10.1016/j.media.2016.01.004>

[37] Bai, W., Sinclair, M., Tarroni, G., Oktay, O., Rajchl, M., Vaillant, G., Lee, A. M., Aung, N., Lukaschuk, E., Sanghvi, M. M., Zemrak, F., Fung, K., Paiva, J. M., Carapella, V., Kim, Y. J., Suzuki, H., Kainz, B., Matthews, P. M., Petersen, S. E., ... Rueckert, D. (2018). Automated cardiovascular magnetic resonance image analysis with fully convolutional networks. *Journal of Cardiovascular Magnetic Resonance*, 20(1). <https://doi.org/10.1186/s12968-018-0471-x>

[38] Karimi-Bidhendi, S., Arafati, A., Cheng, A. L., Wu, Y., Kheradvar, A., & Jafarkhani, H. (2020). Fully-automated deep-learning segmentation of pediatric cardiovascular magnetic resonance of patients with complex congenital heart diseases. *Journal of cardiovascular magnetic resonance : official journal of the Society for Cardiovascular Magnetic Resonance*, 22(1), 80. <https://doi.org/10.1186/s12968-020-00678-0>

[39] Moccia, S., Banali, R., Martini, C., Muscogiuri, G., Pontone, G., Pepi, M. and Caiani, E., 2018. Development and testing of a deep learning-based strategy for scar segmentation on CMR-LGE images. *Magnetic Resonance Materials in Physics, Biology and Medicine*, 32(2), pp.187-195. <https://doi.org/10.1007/s10334-018-0718-4>

[40] Zabihollahy, F., Rajchl, M., White, J., & Ukwatta, E. (2020). Fully automated segmentation of left ventricular scar from 3D late gadolinium enhancement magnetic resonance imaging using a cascaded multi-planar U-Net (CMPU-Net). *Medical Physics*, 47(4), 1645-1655. <https://doi.org/10.1002/mp.14022>

[41] Sander Jörg, de Vos Bob, D., & Išgum Ivana. (2020). Automatic segmentation with detection of local segmentation failures in cardiac MRI. *Scientific Reports (Nature Publisher Group)*, 10(1) <http://dx.doi.org/10.1038/s41598-020-77733-4>

[42] Bai, W., Oktay, O., & Rueckert, D. (2016). Classification of Myocardial Infarcted Patients by Combining Shape and Motion Features. *Statistical Atlases and Computational Models of the Heart. Imaging and Modelling Challenges*, 140–145. https://doi.org/10.1007/978-3-319-28712-6_15

[43] Bai, W., Peressutti, D., Parisot, S., Oktay, O., Rajchl, M., O'Regan, D., Cook, S., King, A., & Rueckert, D. (2016). Beyond the AHA 17-Segment Model: Motion-Driven Parcellation of the Left Ventricle. *Statistical Atlases and Computational Models of the Heart. Imaging and Modelling Challenges*, 13–20. https://doi.org/10.1007/978-3-319-28712-6_2

[44] McGOVERN, B. R. I. A. N., SCHOENFELD, M. A. R. K. H., RUSKIN, J. E. R. E. M. Y. N., GARAN, H. A. S. A. N., & YURCHAK, P. E. T. E. R. M. (1986). Ventricular Tachycardia: Historical Perspective. *Pacing and Clinical Electrophysiology*, 9(3), 449–462. <https://doi.org/10.1111/j.1540-8159.1986.tb04501.x>

[45] *Ventricular Tachycardia Causes and Symptoms*. Ventricular Tachycardia Casues and Symptoms - UChicago Medicine. (n.d.). <https://www.uchicagomedicine.org/conditions-services/heart-vascular/ventricular-tachycardia>.

[46] *Penn Cardiac Electrophysiology*. Home | Penn Cardiac Electrophysiology | Perelman School of Medicine at the University of Pennsylvania. (n.d.). <https://www.med.upenn.edu/ep/>.

[47] *American Heart Association*. www.heart.org. (n.d.). <http://www.heart.org/>.

- [48] European Society of Cardiology. (n.d.). <http://www.escardio.org/>.
- [49] Society for Cardiovascular Magnetic Resonance. (n.d.). <https://www.scmr.org/>
- [50] Heart MRI. (n.d.). <http://www.heartmri.org/>
- [51] Krasnobaev, A., & Sozykin, A. (2016). An Overview of Techniques for Cardiac Left Ventricle Segmentation on Short-Axis MRI. *ITM Web of Conferences* 8, 01003. <https://doi.org/10.1051/itmconf/20160801003>
- [52] Zabihollahy, F., Rajan, S. & Ukwatta, E. Machine Learning-Based Segmentation of Left Ventricular Myocardial Fibrosis from Magnetic Resonance Imaging. *Curr Cardiol Rep* 22, 65 (2020). <https://doi.org/10.1007/s11886-020-01321-1>
- [53] The Global Leader in Cardiac Imaging Solutions. (n.d.). <http://www.circlecvi.com/>
- [54] Medical software solutions. (n.d.). <https://www.medviso.com/>
- [55] Pie Medical Imaging. (n.d.). <https://www.piemedicalimaging.com/>
- [56] Schoenhagen, P., Stillman, A. E., Halliburton, S. S., & White, R. D. (2005). CT of the heart: principles, advances, clinical uses. *Cleveland Clinic Journal of Medicine*, 72(2), 127–138. <https://doi.org/10.3949/ccjm.72.2.127>
- [57] Chan, R. W., Lau, J. Y. C., Lam, W. W., & Lau, A. Z. (2019). Magnetic Resonance Imaging. *Encyclopedia of Biomedical Engineering*, 574–587. <https://doi.org/10.1016/b978-0-12-801238-3.99945-8>
- [58] Eltaller.net. (n.d.). *Fibrosis Imaging for the EP Lab*. ADAS 3D: Fibrosis Imaging for the EP Lab. <https://www.adas3d.com/>.
- [59] Eltaller.net. (n.d.). ADAS 3D. Galgo Medical: ADAS 3D. <https://www.galgomedical.com/en/adas3d.html>.
- [60] Segment CMR. Medviso. (n.d.). <https://medviso.com/cmr/>.
- [61] Software SPSS. IBM. (n.d.). <https://www.ibm.com/es-es/analytics/spss-statistics-software>.
- [62] *Gentle Introduction to Tidy Statistics in R*. RStudio. (2019, June 12). <https://www.rstudio.com/resources/webinars/a-gentle-introduction-to-tidy-statistics-in-r/>.
- [63] BELHASSEN, B., PELLEGG, A., MOTTÉ, G. and LANIADO, S., 1983. Determination of the Left Bundle Branch Refractoriness by Distal His Bundle Pacing in Patients with Left Bundle Branch Block. *Pacing and Clinical Electrophysiology*, 6(6), pp.1245-1251.
- [64] Taylor, A. J., Salerno, M., Dharmakumar, R., & Jerosch-Herold, M. (2016). T1 Mapping. *JACC: Cardiovascular Imaging*, 9(1), 67–81. <https://doi.org/10.1016/j.jcmg.2015.11.005>
- [65] Hindieh, W., Weissler-Snir, A., Hammer, H., Adler, A., Rakowski, H., & Chan, R. (2017). Discrepant Measurements of Maximal Left Ventricular Wall Thickness Between Cardiac Magnetic Resonance Imaging and Echocardiography in Patients With Hypertrophic Cardiomyopathy. *Circulation: Cardiovascular Imaging*, 10(8). <https://doi.org/10.1161/circimaging.117.006309>



[66] Romero, D., Sebastián, R., Plank, G., Vigmond, E., & Frangi, A. (2008). Modeling the influence of the VV delay for CRT on the electrical activation patterns in absence of conduction through the AV node. *Medical Imaging 2008: Visualization, Image-Guided Procedures, And Modeling*. <https://doi.org/10.1117/12.770316>

12. APPENDIX

12.1. Theoretical concepts

The origin of a heartbeat is an electrical stimulus that is generated in the sinus node (SA node), located in the right atrium. This node sends between 60 and 100 electrical pulses every minute, which is the regular heart rate. An electrical pulse travels through the conduction pathways of the heart muscle to the atrioventricular node (AV node), located between the ventricles and the atria. In this node, the impulse is delayed and slowed down for a short instant, which allows the atria to contract just before the ventricles. Thus, the blood from the atria will pass to the ventricles before they contract. Finally, the electrical pulse will continue to travel down through a conduction channel named bundle of His, which bifurcates into two branches that correspond to Purkinje fibers. One branch continues to the right and the other one continues to the left in order to take the electrical stimuli to the rest of both right and left ventricle.

Cardiac arrhythmias are heart rhythm disorders caused by atypical electric signals that lead to abnormal heart rhythms such as bradycardias (too slow heart rate), tachycardias (too fast heart rate) or too irregular heart rate. Bradycardias can be treated with pacemakers but, regarding the treatment for tachycardias, an antiarrhythmic therapy, a surgical ablation or even an implantable cardioverter-defibrillator therapy can be considered for the patient depending on its clinical status, indications or complications. Thus, an exhaustive study of the patient's situation will be needed in order to treat them accurately.

This study is focused specially on ventricular tachycardia, which is characterized by the abnormal heartbeat of the cardiac muscle since the SA node does not control the beat of the ventricles anymore because other parts of the lower conduction path take over the role of pacemaker. This irregular rhythm makes the patient feel palpitations and it can lead to short of breath, dizziness or fainting among other symptoms and conditions. There are mainly four types of VT:

- **Ventricular extrasystoles or premature ventricular contractions:** it consists of an impulse that has its origin in an isolated point of the ventricle, and it anticipates the regular rhythm of the rest of the ventricle. This condition is not usually treated since it is not dangerous, but it can be treated pharmacologically with beta blockers if necessary.
- **Sustained-VT:** it is characterized by a series of ventricular impulses causing an important increase in heart rate for more than 30 seconds. If these impulses do not cease, it will be necessary to treat them with antiarrhythmic drugs or performing an electrophysiological study in order to plan an accurate and effective ablation to terminate the origin of the VT. Moreover, if risk of sudden death is suspected, an implantation of an ICD (implantable cardioverter-defibrillator) will be needed.
- **Non-sustained VT:** this condition involves a series of ventricular impulses for less than 30 seconds that cease eventually spontaneously.
- **Ventricular fibrillation (VF):** this alteration disorganizes completely the ventricular impulses until there is not a specific or repetitive electrical activation pattern, so the heartrate increases up to 300 beats per minute, but the heart is not able to produce any effective heartbeat. Different symptoms such as no pulse and immediate loss of consciousness are involved in this condition. If it is not treated on time, it can result on death in a few minutes.

Myocardial cells are specialized on the mechanical contraction of the heart and on its electrical impulses. These type of cells own three important electrical properties; the automatism, which is the ability to automatically generate an action potential that will arrive to a certain threshold so

that cardiac contraction can be generated, the excitability, capacity to respond to electrical and mechanical stimuli and depolarise and the conductivity, which represents the transmission of these depolarisations between cells. The propagation of the cardiac impulse is possible due to gap unions, structures formed by different ionic intracellular channels that supply the electric communication between the cells and, since each cardiac cell expresses different types and number of cells, the action potential will show differences depending on the region.

For a contractile response to develop, an electric response in the membrane called action potential has to be generated. The ventricular action potential for cardiomyocytes develops with the following phases.

- **Phase 4:** resting potential, about -90mV.
- **Phase 0:** rapid depolarization as a consequence of a massive inlet of Na⁺ ions through the voltage-gated Na⁺ channels. Then, these channels become inactive, in a refractory period.
- **Phase 1:** partial repolarization because of a decrease in sodium ions since Na⁺ channels close.
- **Phase 2:** plateau phase. It is a long phase in which the calcium enters into the cell because the Ca⁺⁺ channels open and the influx of Ca⁺⁺ triggers the depolarization.
- **Phase 3:** rapid repolarization. Na⁺ and Ca⁺⁺ channels are all closed, K⁺ channels open and membrane potential returns to its resting value.

The pacemaker cells set the rate of the heart and they generate action potentials spontaneously. They are characterized by not contributing to the contractile force of the heart. As mentioned before, the SA node is the main and fastest pacemaker, so it has an essential role in initiating diastolic depolarisation.

12.2. Tables used to compute *Figure 33*

AHA1

		Frecuencia	Porcentaje	Porcentaje válido	Porcentaje acumulado
Válidos	NO	75	24,1	94,9	94,9
	SÍ	4	1,3	5,1	100,0
	Total	79	25,4	100,0	
Perdidos	Sistema	232	74,6		
Total		311	100,0		

AHA2

		Frecuencia	Porcentaje	Porcentaje válido	Porcentaje acumulado
Válidos	NO	76	24,4	96,2	96,2
	SÍ	3	1,0	3,8	100,0
	Total	79	25,4	100,0	
Perdidos	Sistema	232	74,6		
Total		311	100,0		



AHA3

		Frecuencia	Porcentaje	Porcentaje válido	Porcentaje acumulado
Válidos	NO	70	22,5	88,6	88,6
	SÍ	9	2,9	11,4	100,0
	Total	79	25,4	100,0	
Perdidos	Sistema	232	74,6		
Total		311	100,0		

AHA4

		Frecuencia	Porcentaje	Porcentaje válido	Porcentaje acumulado
Válidos	NO	68	21,9	86,1	86,1
	SÍ	11	3,5	13,9	100,0
	Total	79	25,4	100,0	
Perdidos	Sistema	232	74,6		
Total		311	100,0		

AHA5

		Frecuencia	Porcentaje	Porcentaje válido	Porcentaje acumulado
Válidos	NO	72	23,2	91,1	91,1
	SÍ	7	2,3	8,9	100,0
	Total	79	25,4	100,0	
Perdidos	Sistema	232	74,6		
Total		311	100,0		

AHA6

		Frecuencia	Porcentaje	Porcentaje válido	Porcentaje acumulado
Válidos	NO	77	24,8	97,5	97,5
	SÍ	2	,6	2,5	100,0
	Total	79	25,4	100,0	
Perdidos	Sistema	232	74,6		
Total		311	100,0		



AHA7

		Frecuencia	Porcentaje	Porcentaje válido	Porcentaje acumulado
Válidos	NO	67	21,5	84,8	84,8
	SÍ	12	3,9	15,2	100,0
	Total	79	25,4	100,0	
Perdidos	Sistema	232	74,6		
Total		311	100,0		

AHA8

		Frecuencia	Porcentaje	Porcentaje válido	Porcentaje acumulado
Válidos	NO	72	23,2	91,1	91,1
	SÍ	7	2,3	8,9	100,0
	Total	79	25,4	100,0	
Perdidos	Sistema	232	74,6		
Total		311	100,0		

AHA9

		Frecuencia	Porcentaje	Porcentaje válido	Porcentaje acumulado
Válidos	NO	62	19,9	78,5	78,5
	SÍ	17	5,5	21,5	100,0
	Total	79	25,4	100,0	
Perdidos	Sistema	232	74,6		
Total		311	100,0		

AHA10

		Frecuencia	Porcentaje	Porcentaje válido	Porcentaje acumulado
Válidos	NO	58	18,6	73,4	73,4
	SÍ	21	6,8	26,6	100,0
	Total	79	25,4	100,0	
Perdidos	Sistema	232	74,6		
Total		311	100,0		

AHA11

		Frecuencia	Porcentaje	Porcentaje válido	Porcentaje acumulado
Válidos	NO	67	21,5	84,8	84,8
	SÍ	12	3,9	15,2	100,0
	Total	79	25,4	100,0	
Perdidos	Sistema	232	74,6		
Total		311	100,0		



AHA12

		Frecuencia	Porcentaje	Porcentaje válido	Porcentaje acumulado
Válidos	NO	76	24,4	96,2	96,2
	SÍ	3	1,0	3,8	100,0
	Total	79	25,4	100,0	
Perdidos	Sistema	232	74,6		
Total		311	100,0		

AHA13

		Frecuencia	Porcentaje	Porcentaje válido	Porcentaje acumulado
Válidos	NO	67	21,5	84,8	84,8
	SÍ	12	3,9	15,2	100,0
	Total	79	25,4	100,0	
Perdidos	Sistema	232	74,6		
Total		311	100,0		

AHA14

		Frecuencia	Porcentaje	Porcentaje válido	Porcentaje acumulado
Válidos	NO	61	19,6	77,2	77,2
	SÍ	18	5,8	22,8	100,0
	Total	79	25,4	100,0	
Perdidos	Sistema	232	74,6		
Total		311	100,0		

AHA15

		Frecuencia	Porcentaje	Porcentaje válido	Porcentaje acumulado
Válidos	NO	56	18,0	70,9	70,9
	SÍ	23	7,4	29,1	100,0
	Total	79	25,4	100,0	
Perdidos	Sistema	232	74,6		
Total		311	100,0		

AHA16

		Frecuencia	Porcentaje	Porcentaje válido	Porcentaje acumulado
Válidos	NO	64	20,6	81,0	81,0
	SÍ	15	4,8	19,0	100,0
	Total	79	25,4	100,0	
Perdidos	Sistema	232	74,6		
Total		311	100,0		



AHA17

		Frecuencia	Porcentaje	Porcentaje válido	Porcentaje acumulado
Válidos	NO	74	23,8	93,7	93,7
	SÍ	5	1,6	6,3	100,0
	Total	79	25,4	100,0	
Perdidos	Sistema	232	74,6		
Total		311	100,0		